TOPICAL REVIEW • OPEN ACCESS

2D materials: advances in regenerative medicine and human health sensing

To cite this article: Jasmina Lazarević and Bojana Višić 2025 *2D Mater.* **12** 042001

2D Materials

TOPICAL REVIEW

2D materials: advances in regenerative medicine and human health sensing

Jasmina Lazarević[1] and Bojana Višić[1,2,*]

[1] Center for Solid State Physics and New Materials, Institute of Physics Belgrade, University of Belgrade, Pregrevica 118, Belgrade 11080, Serbia
[2] Department of Condensed Matter Physics, Jozef Stefan Institute, Jamova cesta 39, Ljubljana 1000, Slovenia
* Author to whom any correspondence should be addressed.

E-mail: bojana.visic@ijs.si

Keywords: 2D materials, humidity sensing, wearable sensors, transition-metal dichalcogenides, biological activity, regenerative medicine

OPEN ACCESS

RECEIVED
3 April 2025

REVISED
19 June 2025

ACCEPTED FOR PUBLICATION
30 July 2025

PUBLISHED
12 August 2025

Abstract

The potential of 2D materials goes beyond the use in electronic applications, extending to regenerative medicine and noninvasive sensing. They hold great promise in these fields due to their remarkable properties, such as high surface area, electrical conductivity and modular chemistry. However, they face significant challenges related to biocompatibility, long-term safety, reproducible large-scale production and lack of standardization and clinical protocols, among others. This review presents a comprehensive overview of their application in regenerative medicine and interactions with various biological systems. We comment on the influence of their innate, but tunable properties on biological response. The chemical composition and exfoliation state of these materials also play a critical role in their bioactivity. The high sensitivity of 2D materials to humidity holds a significant promise in sensor development, which is presented here in detail. Combining them with polymer matrices can enhance the flexibility and performance of the sensors, making them suitable for wearable devices and environmental monitoring. However, challenges remain in the search for the best sensing characteristics, which can be addressed through functionalization and combining with alternative materials like metal oxide nanowires. We critically examined the key challenges (biological interactions, exposure risks, environmental changes and scalability), while assessing their potential for sustainable technologies. Despite the advancements, thorough safety assessments are needed before large-scale production and clinical deployment of 2D materials for health sensing applications.

1. Introduction

The vast, diverse and complex field of 2D materials affects nearly every aspect of life, with applications extending far beyond electronics to energy storage, coatings, cosmetics, food industry and biomedicine. Their biological and environmental interactions are of particular significance, as both living organisms and entire ecosystems ultimately become end users, whether through intentional applications or unintended exposure. Factors such as size, shape and surface characteristics of nanomaterials significantly influence the extent of their stability. These transformations can alter their physicochemical properties, which may, in turn, affect their environmental interactions and potentially modify their toxicity.

There is a notable dominance of high-quality research papers on graphene and its derivatives, likely because they were the first and most extensively studied group of 2D materials. However, inorganic layered materials, particularly MoS_2, have attracted increasing research attention into their bioactivity. In chapter 2, we discuss the recent application advances in regenerative medicine, including cardiac, neural and bone tissue regeneration from the perspective of the materials, emphasizing their functional roles while integrating both physical

principles and biological relevance. We also comment on related topics such as drug delivery, organoid culture, angiogenesis, adipogenesis and phototherapy. Composite materials were mentioned only where necessary to emphasize the specific functionalities of 2D materials, such as improving mechanical strength, electrical conductivity or biological performance relevant to regenerative applications.

The field of noninvasive sensing has been increasingly popular due to a variety of possibilities for applications, such as e-skin [1], touchless interfaces, skin patches etc. For example, skin patches can be used to monitor different types of vital human health information. Tracking the levels of humidity of human skin in real-time can provide a variety of crucial information about the health status, such as wound healing, metabolic conditions and effectiveness of cosmetic products [2]. The search for a sensor with high sensitivity, wide detection range, quick response and short recovery time is moving into the area of novel 2D materials. One of the major challenges is to achieve high and even sensitivity for the full range of humidity. 2D materials hold a lot of potential, as their high surface-to-volume ratio allows for better sensitivity to humidity changes. In chapter 3, we review the recent progress in the fabrication of humidity sensors based on 2D materials. Their performance for monitoring human breath, touch, or humidity in agriculture is discussed in chapters 4 and 5. In chapter 6, we have critically addressed key challenges of application of 2D materials, including their interactions with biological systems, exposure risks, environmental transformations, and limitations in scalability and stability, while also evaluating their potential in sustainable technologies. Finally, the last chapter focuses on the future perspectives and mitigation strategies necessary to advance these fields further.

2. 2D materials in regenerative medicine

With the world population getting older, modern medicine aims to restore tissues and organs damaged by injuries, illnesses, aging or congenital abnormalities, with stem cells (SCs) playing a key role in regenerative therapies due to their ability to self-renew, differentiate into tissue specific cells, immunomodulation properties and secretion of paracrine factors [3, 4]. Their inherent plasticity enables precise response to external cues and adoption of specific lineages. From a clinical standpoint, while embryonic SCs (ESCs) and induced pluripotent SCs (iPSCs) offer the highest differentiation potential due to their pluripotency, their use presents significant challenges. ESCs raise ethical concerns related to their isolation, while both ESCs and iPSCs carry risks of uncontrolled differentiation, tissue overgrowth and teratoma formation. On the other hand, adult SCs, such as mesenchymal SCs (MSCs), are multipotent and widely studied due to the ease of their isolation and absence of ethical concerns [5]. It is of utmost importance to ensure SCs survival during transplantation and *in vivo* for the success of regenerative medicine approaches. Beyond regenerative medicine, MSCs serve as valuable models in drug development, offering physiologically relevant alternatives to immortalized cell lines and minimizing dependence on animal testing [6]. Given their lifelong presence, ensuring MSCs survival and functionality is crucial for both regenerative and toxicological research [7].

Although at the forefront as a tool for treating currently incurable medical conditions, SCs still need a little encouragement, and this is where 2D materials come into play. Materials reviewed in this paper, as well as their role in the field of regenerative medicine, are summarized in table 1. They offer not only physical scaffolding for transplanted cells but also actively modulate the biological microenvironment to enhance cellular responses. By mimicking key features of the native extracellular matrix (ECM), such as surface topography, stiffness and biochemical cues, 2D materials can significantly improve SC adhesion, proliferation, and lineage-specific differentiation [8, 9]. Their high surface area and tunable surface chemistry facilitate the adsorption and presentation of growth and differentiation factors, making them powerful tools for directing SC fate. The interaction at the cell-material interface, being the initial point of contact, is crucial. Nanoscale surface features of 2D materials promote focal adhesion formation and cytoskeletal reorganization, both of which are essential for mechanotransduction pathways that drive differentiation. Therefore, the integration of 2D materials into regenerative platforms holds great promise for advancing SC-based therapies by providing structural support and biological guidance within the physiologically relevant environments.

2.1. 2D materials in cardiac regeneration and angiogenesis

Regenerative strategies offer the most promising long-term solutions for cardiovascular diseases, which are the leading cause of death globally, according to the World Health Organization. They are utilizing biomaterial-based scaffolds, SCs and growth factors to repair damaged cardiac tissue, although surgical and pharmacological treatments are still the first line methods. The effectiveness of 2D materials in this context depends on their physicochemical properties, such as high electrical conductivity and surface to volume ratio, mechanical strength and flexibility; biocompatibility and immunomodulatory capabilities [8, 9].

According to the literature, graphene and its derivatives, such as graphene oxide (GO) and reduced GO (rGO), are among the most extensively studied

Table 1. The summary of 2D materials discussed in this paper, their key features and the application in regenerative medicine.

2D material	Key characteristics	Role in regenerative medicine
Graphene oxide (GO)	High surface area; oxygenated functional groups; tunable electrical conductivity	Promotes osteogenesis, enhances angiogenesis, supports stem cell proliferation and differentiation in bone tissue scaffolds, neural tissue regeneration
Reduced graphene oxide (rGO)	Conductive; lower oxygen content; excellent mechanical reinforcement	Enhances osteoblast differentiation, mineralization; supports bone formation *in vivo,* scaffold for neural tissue regeneration
MXenes (e.g. $Ti_3C_2T_x$)	Metallic conductivity; hydrophilic; antioxidant (ROS scavenging); electrically conductive	Creates conductive hydrogel scaffolds for cardiac repair, supports tissue adhesion and cardiomyocyte function
Transition metal dichalcogenides (e.g. MoS_2, WS_2)	Semiconducting; photothermal properties; good biocompatibility	Promotes MSC adhesion and osteogenic differentiation; used in skin, bone and nerve regeneration
Hexagonal boron nitride (h-BN)	Chemically inert; high thermal and mechanical stability	Supports both osteogenic and adipogenic differentiation; neural tissue regeneration

materials, with a wide range of applications in modern medicine. These include their use as scaffolds and guidance materials in regenerative medicine, components in biosensors, as neural interface devices and brain implants, some of which have already entered clinical trial phases [10, 11]. They provide an excellent surface for cell attachment and proliferation, particularly for MSCs and cardiomyocytes, as shown in figure 1. The extent to which GO affects SC behavior is highly dependent on several factors, including concentration, exposure time and surface modifications. Studies suggest that altering the physicochemical properties of GO, such as functionalization with biocompatible coatings, could mitigate some of its adverse effects. In addition to the mechanical support that promotes cell differentiation and consequently, tissue regeneration and functional repair, graphene and its derivatives also guide and enhance differentiation of MSCs towards specific cardiac cell types due to their electrical features [12, 13]. Namely, these materials possess extraordinary electrical conductivity across large surface area which facilitates cell-to-cell communication and maturation by the upregulation of key cardiac markers, such as connexin 43 (a gap junction protein crucial for electrical coupling) and cardiac-specific genes, thereby enhancing the differentiation process. Moreover, the surface of GO, rich in oxygen-containing functional groups, promotes strong interactions with ECM proteins, improving SC adhesion, proliferation and survival. These interactions protect MSCs from oxidative stress and enhance their paracrine signaling, contributing to angiogenesis and tissue repair when transplanted to infracted myocardium [14, 15]. Through these mechanisms, graphene-based materials not only guide SCs differentiation, but also ensure better integration and functionality of the newly formed cardiac tissues, offering promising strategies for cardiac tissue engineering and regenerative therapies. The conductivity of graphene closely resembles that of the native myocardium, which allows these scaffolds to effectively transmit electrical signals between cardiomyocytes, promoting synchronized contractions and improved tissue integration. Myogenic scaffolds require higher conductivity and mechanical robustness to facilitate rhythmic, force-generating contractions, whereas neurogenic scaffolds prioritize directional growth, synapse formation, and moderate signal transmission support [13]. Functionalized graphene derivatives (e.g. GO functionalized with peptides or proteins) further improve cell adhesion, viability, and differentiation into cardiac-like cells by mimicking physiological conditions in ECM [16, 17]. It was observed that graphene-coated surfaces promote cardiomyocyte alignment, mimicking the native structure of heart tissue, which is crucial for functional integration. However, recent findings of Heo *et al* [18] indicate that GO may have unintended consequences when interacting with human iPSCs generated from fibroblasts. This raises concerns about its suitability for regenerative medicine applications. One of the most critical observations is that exposure to GO of varying lateral sheet sizes (in average 150 nm, 400 nm and 1 μm) and concentrations appears to interfere with key molecular pathways that sustain pluripotency [18]. Human iPSCs rely on a strictly regulated microenvironment to maintain their undifferentiated state, and any disruption to this balance can lead to premature lineage commitment. In this study, when cultured in cardiomyocyte induction medium, the upregulation of cardiomyocyte marker NKS2.5 was evidenced. This premature differentiation is a significant challenge, as maintaining precise control over SC behavior is

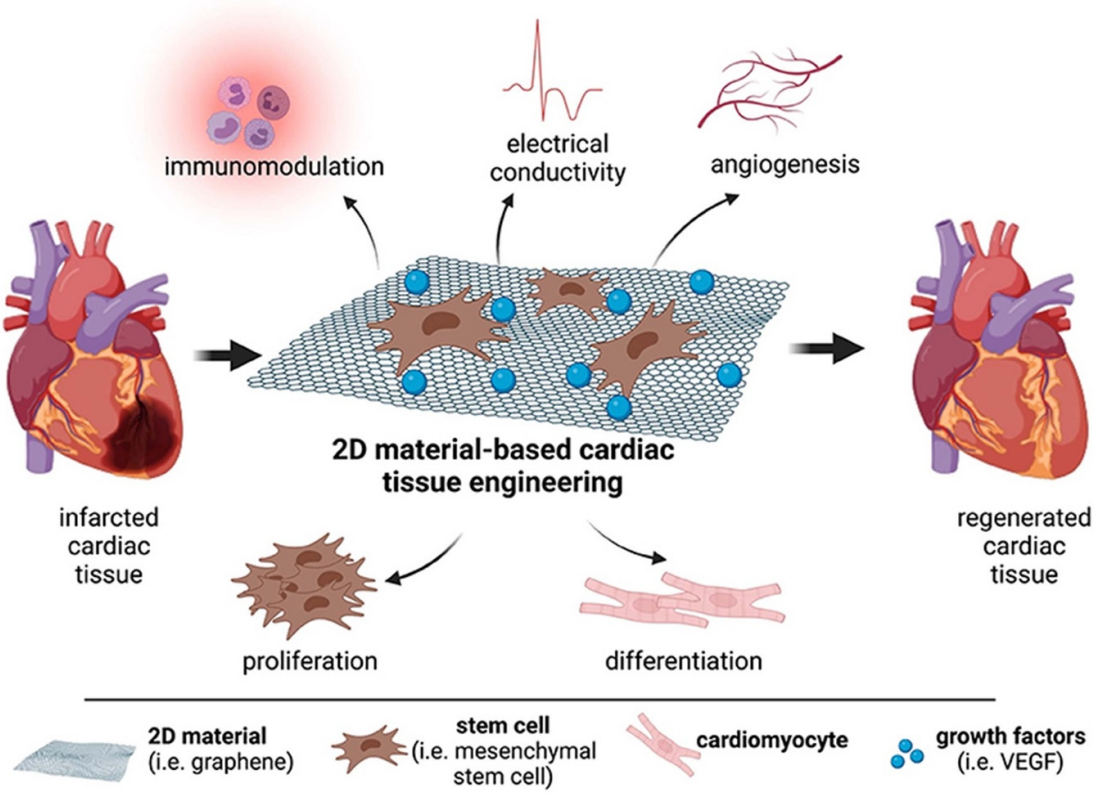

Figure 1. The potential of 2D materials for cardiac repair and regeneration. Graphene or graphene derivatives can act as scaffolds for MSCs and deliver growth factors to the infracted area. Reproduced from [8]. CC BY 4.0.

essential for their successful application in regenerative therapies. When intentional, the ability to interfere with differentiation is valuable, but in this case, the lack of control could undermine the reliability of GO as a biomaterial for SC-based treatments. Additionally, GO increased both reactive oxygen species (ROSs) and caspase-3 activity as a result from cellular uptake initializing apoptotic signal in concentration of 100 μg ml^{-1}. The hiPSCs lost their pluripotency, based on significant loss in pluripotency markers OCT-4 and NANOG regardless the lateral sheet size.

GO-based 3D scaffolds (including pure and functionalized GO) provide structural support that enhances cell proliferation, differentiation and tissue formation, making them particularly valuable in regenerative medicine and organoid development [19, 20]. They offer several advantages over Matrigel, which is derived from mouse tumor ECM and shows batch-to-batch variability, undefined composition and presence of xenogeneic contaminants. GO-based scaffolds have been used in organoid cultures to create disease models that closely resemble *in vivo* conditions and are essential for studying disease mechanisms, testing new drugs and understanding tissue responses to different treatments. In a recent study, 3D liver organoids (LOs) composed of upcyte® human hepatocytes, liver sinusoidal endothelial cells, and mesenchymal stromal cells were repeatedly exposed to GO at concentrations of 2–40 μg ml^{-1}. While the LOs maintained overall viability and structural integrity, they showed a downregulation of CYP3A4 expression, suggesting potential disruption of hepatic metabolic function [21]. These findings point out the value of LOs as physiologically relevant *in vitro* models for evaluating the long-term and cumulative effects of nanomaterials, especially under conditions resembling real-life exposure scenarios. Due to its bio functional properties, GO can also act as a drug delivery system, allowing controlled and targeted drug release in cancer therapy and regenerative applications.

The recent study by Yu *et al* highlights MXene-incorporated hydrogels as a promising platform for functional cardiac regeneration following an ischemic injury [22]. A $Ti_3C_2T_x$ MXene-based hydrogel was developed by incorporating MXene nanosheets into a GelMA–PANI matrix, achieving conductivity of 0.23 S m^{-1} and a compressive modulus of ~35 kPa, closely mimicking native myocardial tissue. *In vitro*, neonatal rat cardiomyocytes cultured on the hydrogel showed enhanced viability, spreading, and expression of cardiac-specific markers (cTnT, α-actinin, connexin-43), along with synchronous contractions and improved calcium signaling. *In vivo,* MXene hydrogel treatment led to significant functional

recovery, with increases in ejection fraction (16.5%) and fractional shortening (12.8%), alongside reduced infarct size, fibrosis, and increased angiogenesis. Immunofluorescence showed better tissue preservation and cellular alignment. The MXene component also provided antioxidative and anti-inflammatory effects by scavenging ROS and reducing TNF-α and IL-6 expression. The hydrogel biodegraded over 4 weeks, aligning with tissue healing.

Enhancing angiogenesis, as focal point in tissue engineering and SC therapy, can improve the success of transplanted tissues and the repair of damaged organs, like the heart after a myocardial infarction. GO and rGO materials significantly influence the angiogenic differentiation of hUC-MSCs [12, 23]. Cells cultured on large GO flakes demonstrated a notable increase in the expression of angiogenic markers such as GATA-2, endoglin and VE-cadherin. The expression levels were up to 3.5 times higher compared to cells grown on standard culture surfaces. Interestingly, the differentiation medium did not enhance this effect further, indicating that the GO-lf surface itself played a critical role in promoting angiogenic differentiation. Additionally, cells cultured on rGO-lr-P60 surfaces (a slightly reduced form of rGO) exhibited significantly elevated expressions of angiogenic markers, particularly GATA-2, which showed a 110-fold increase in expression compared to standard culture surfaces. The promotion of angiogenesis was further supported by functional assays, where hUC-MSCs demonstrated enhanced capillary tube formation on GO and rGO surfaces, indicating improved proangiogenic capabilities.

2.2. 2D materials in bone tissue regeneration

Bone tissue engineering aims to develop materials that surpass traditional bone autografts and allografts and the process must be finely tunable and dynamic as osteogenesis and bone remodeling physiologically are. Materials used must account for age-related changes in bone microstructure and diminished regenerative capacity for elderly patients and, in contrast, pediatric applications require materials with adaptable structural properties or those that facilitate remodeling to support skeletal growth. Additionally, sex-related differences in bone microstructure and size further emphasize the need for personalized approaches. In natural bone, bioelectrical signals such as piezoelectricity, ferroelectricity and pyroelectricity are generated in response to mechanical stress, polarization and temperature variations, respectively. These signals play a crucial role in regulating cellular activities essential for bone healing, remodeling and growth [24, 25]. Piezoelectricity, produced by the deformation of collagen and other structural components, generates localized electrical charges that influence osteoblast function and guide SC differentiation toward bone-forming pathways. Ferroelectricity, which involves reversible spontaneous polarization under an external electric field, provides continuous electroactive signals that support bone matrix mineralization. Arising from temperature-induced potential changes, pyroelectricity introduces additional electrical stimuli that may be particularly relevant during inflammatory responses or thermal fluctuations following injury. These mechanisms form a dynamic bioelectrical environment that is integral to bone regeneration and scaffolds should not only structurally support but also [24] generating bioelectrical stimuli to promote tissue regeneration. Moreover, scaffold materials in bone tissue engineering are designed to gradually degrade and be replaced by newly formed tissue that closely replicates the mechanical properties of native bone. This ensures that the regenerated bone can provide the necessary strength, stability and functionality required for long-term integration within the body. When it comes to osteogenesis, it was demonstrated that graphene can promote the osteogenic differentiation of hMSCs even without a key growth factor in bone formation, BMP-2 [26, 27]. Higher calcification was observed by alizarin red staining in the presence of graphene. Additionally, variations in osteogenesis were noted depending on the presence or absence of both graphene and BMP-2. This effect is attributed to the localized accumulation of osteogenic molecules, such as dexamethasone and β-glycerophosphate, facilitated by non-covalent interactions like π–π stacking with the graphene surface [28]. A single layer GO at low doses increases the roughness and decreases the stiffness of the alginate hydrogels in which single human BMSCs have been encapsulated, as indicated by microfluidics-based approach. This enhances cell viability, proliferation and osteogenic differentiation and thus, offers a promising approach for minimally invasive injectable bone tissue transplants [29]. When Raw264.7 cells were cultured on bioactive glass/GO scaffolds, GO significantly facilitated the polarization of macrophages toward the M2 phenotype, promoting the secretion of osteogenic and angiogenic factors. This, in turn, enhanced the osteogenic differentiation of rat BMSCs and stimulated angiogenesis in endothelial cells [19]. The degradation rate of the scaffold is carefully tuned, combined with biopolymers like collagen and gelatin, to align with the pace of natural bone regeneration, preventing structural deficiencies while promoting seamless tissue remodeling [26, 30, 31]. Furthermore, 3D printed composite materials that include GO and polycaprolactone (PCL) are designed as scaffolds for application in wound healing and tissue engineering, encompassing its mechanical strength with biological functionality. In GO-PCL composite, GO adds strong antibacterial properties, disrupting bacterial membranes

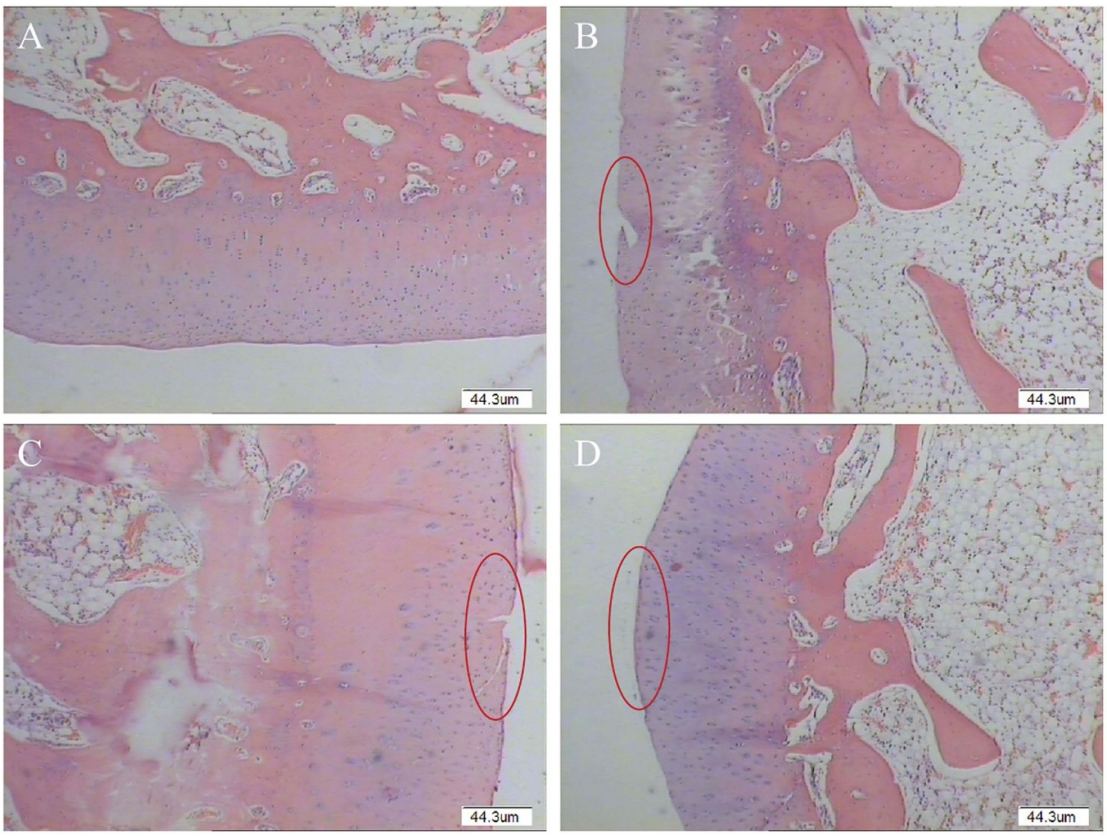

Figure 2. Patho-histological observation results of modified papain release joint injection group. (A) Blank, (B) GO group, (C) UCMSCs group, (D) GO + UCMSCs group. Red circle denotes cartilage erosion area. Reproduced from [33]. CC BY 4.0.

and inducing oxidative stress, minimizing in that way the risk of bacterial infection during the healing process [32]. On the other hand, its low cytotoxicity and high biocompatibility enhance its potential for various applications. Importantly, umbilical cord-derived MSCs (hUC-MSCs) loaded with GO granular lubricant can enhance chondrocyte secretion, lower joint inflammation, improve subchondral bone osteoporosis and support cartilage regeneration in knee osteoarthritis animal models (see figure 2) [33]. GO serves as a multifunctional reinforcing agent that not only strengthens the scaffold mechanically but also amplifies its bioelectrical functionality. When incorporated into polyvinylidene fluoride (PVDF) scaffolds produced by selective laser sintering, GO significantly promotes the transformation of the polymer's α phase to the electroactive β phase [34]. This is achieved through strong hydrogen bonding between the oxygen-containing groups of GO and the fluorine atoms in PVDF, which induces chain alignment favorable to β-phase formation. As a result, the PVDF/0.3GO scaffold demonstrated a marked increase in piezoelectric performance, achieving an output voltage of ~8.2 V and current of ~101.6 nA—improvements of 82.2% and 68.2%, respectively, compared to pure PVDF. In addition to enhancing electrical output, GO also reinforced the scaffold mechanically, leading to a 97.9% increase in compressive strength and a 24.5% increase in tensile strength. These improvements are attributed to the strong interfacial interactions between GO and the PVDF matrix. Furthermore, *in vitro* studies confirmed that the enhanced electrical activity positively influenced cell behavior.

Transition metal dichalcogenides (TMDs) offer key advantages over graphene and its derivatives in regenerative medicine, primarily due to their intrinsic semiconducting properties and photothermal/photodynamic capabilities. Unlike graphene, which lacks a bandgap, TMDs enable light-responsive and electrically regulated applications, such as controlled drug release and phototherapy which enhance cell behavior and tissue repair [35]. Their broader chemical diversity, stimuli-responsiveness and ability to support cell differentiation without extensive functionalization make them especially attractive for developing smart, bioactive scaffolds. Molybdenum disulfide (MoS_2) promotes osteogenic differentiation of hMSCs by facilitating the adsorption of differentiation-inducing factors, enhancing cell adhesion and promoting differentiation into osteoblasts by upregulating osteogenic marker genes. This was confirmed through various assays, including optical microscopy and alizarin red S staining, which

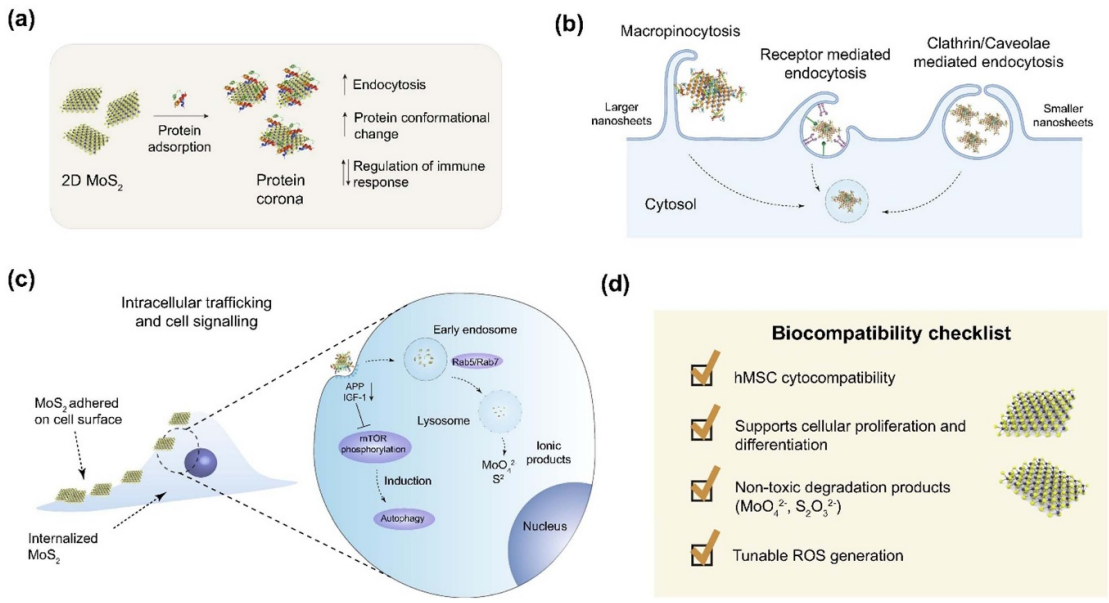

Figure 3. MoS_2-protein interactions, cellular uptake and biocompatibility. (a) Internalization of 2D MoS_2 nanosheets with proteins result in the formation of a protein corona on the surface of the nanosheets, which regulates different cellular processes like nanosheet uptake, protein function and regulation of immune response. (b) Size dependent cellular uptake of 2D MoS_2 nanosheets occurs through micropinocytosis or endocytosis. Presence of corona also facilitates receptor mediated endocytosis. (c) Intracellular trafficking of 2D MoS_2 nanosheets through endo-lysosomal pathway leads to its degradation into ionic products. (d) Biocompatibility checklist of 2D MoS_2 nanosheets. Reprinted from [37], Copyright (2022), with permission from Elsevier.

highlighted significant mineralization, a fingerprint of osteogenic differentiation. Furthermore, gene expression analysis validated the upregulation of key osteogenic marker genes, indicating that MoS_2 effectively supports the osteogenic lineage. Adversely, it has minimal influence on adipogenic differentiation. Due to its photothermal properties, light-mediated modulation of SCs behavior can further influence differentiation outcomes [36]. Similar to MoS_2, tungsten-sulfide's (WS_2) surface properties enhanced the adhesion of hMSCs and facilitated their differentiation into osteocytes with minimal or no influence over adipogenesis. Both of these materials possess strong in-plane covalent bonds and weak out-of-plane van der Waals interactions, with surface roughness that promotes interactions between cells and surface, tunable for optimization. Moreover, both of these materials show minimal cytotoxicity [27]. In SC research, MoS_2 nanosheets provide biophysical stimuli that enhance adhesion, proliferation and differentiation. Their nanostructured surfaces mimic extracellular matrices, improving cytoskeletal organization and focal adhesion formation, as shown in figure 3 [37]. Biomolecule corona on MoS_2 nanosheets that dictates its biological interaction and compatibility is, unlike in graphene-protein interactions, the consequence of van der Waals energies and electrostatic interactions that regulates the conformation of the adsorbed protein [36]. That initial interaction with proteins allows cellular uptake, intracellular trafficking and immune responses. Cellular uptake of MoS_2 occurs mainly via endocytosis, influenced by factors like nanosheet size, surface chemistry and functionalization. Furthermore, MoS_2 nanoflowers exhibits interactions with immune cells, such as macrophages and dendritic cells, modulating immune responses, leaving the space to be used as drug delivery vehicle for immunomodulation [38]. It can promote pro-inflammatory responses at higher concentrations but also shows potential in immunomodulation strategies. The *in vivo* formation of a biomolecular corona on nanoparticles (NPs) has only recently been recognized as a critical advancement in the field of nanomedicine, facilitating a range of significant biomedical applications, including the modulation of immune responses, targeted delivery through endogenous pathways and the scavenging of disease-associated biomarkers [39].

On the other hand, boron nitride (BN) as a chemically inert, thermally conductive and electrically insulating 2D material with excellent mechanical strength supported both, osteogenic differentiation and adipogenesis, but with significantly higher potential for adipogenesis, which was proved with oil red O staining and significantly elevated expression levels of adipogenic marker genes. This is explained by favoring the adsorption of adipogenic-inducing factors and relatively smoother surface which provides less mechanical stimulation and promotes lower cytoskeletal tension and rounded cell shape characteristic for adipogenesis. Moreover, BN stimulates adipogenesis-related signaling pathways like such as

the PPARγ and C/EBPα while providing insufficient mechanical or biochemical stimuli to effectively trigger osteogenic differentiation [40, 41].

2D metal carbides and nitrides (MXenes), known for their exceptional electrical conductivity, play a significant role in promoting the growth and differentiation of electrically active tissues, such as neural and cardiac tissues. Strong interlayer interactions in MXenes yield a stable aqueous colloidal suspension which allows endurance and lower cytotoxicity in biological environment [42]. Through the combined effects, photoactivated MXene promotes bone and soft tissue repair at the same time [43]. The photoactivation of MXene nanosheets ($Ti_3C_2T_x$), which converts light into localized heat, occurs through the absorption of near-infrared (NIR) light (808 nm). This photothermal activation enhances the antibacterial properties of MXene, generating sufficient heat to expose antibacterial effect on pathogenic bacteria, including methicillin-resistant *S. aureus*. The photoactivation also stimulates angiogenesis by upregulating pro-angiogenic factors (such as VEGF) while promoting cell migration and proliferation, accelerating wound healing. Moreover, MXene exposed to NIR light indirectly activates ERK signal pathway in adipose-derived SCs *in vitro*, elevating calcium mineralization by improving the activity of alkaline-phosphatase, driving osteogenic differentiation. Despite their promising potential in healthcare, MXenes face several limitations that must be addressed for successful biological application. Their tendency to oxidize in physiological environments compromises stability and functionality over time. Additionally, concerns regarding cytotoxicity, inconsistent surface terminations and unpredictable interactions with biological media raise challenges in ensuring biocompatibility and safety. The complexity of their synthesis, often involving harsh chemicals, further limits scalability and clinical translation. Therefore, comprehensive *in vivo* studies and standardized protocols are essential to fully realize MXenes' potential in biomedical settings [44]. In addition to their electrical properties, MXenes show remarkable mechanical robustness, making them ideal candidates for reinforcing scaffolds designed for load-bearing tissues, such as bone and cartilage. Their mechanical strength enhances scaffold stability, supports cellular integration and ensures better structural integrity during tissue formation.

2.3. 2D materials in neural tissue regeneration

Neural repair and regeneration are inherently slow and limited processes, particularly within the central nervous system, where neurons have a restricted ability to regenerate after injury. This limited regenerative capacity is due to factors such as inhibitory environments, the formation of scar tissue, and the complex structure of neural networks, which altogether obstruct the restoration of normal neural function [45]. Graphene-based scaffolds have demonstrated promising potential in promoting neuronal regeneration, particularly for repairing peripheral nerve injuries. In an extensive 18 month rat study, these scaffolds exhibited low toxicity, with no significant adverse effects observed in major organs such as the liver, kidneys, heart, lungs or spleen [46, 47]. These scaffolds effectively supported myelination, axonal growth and improved both locomotor and electrophysiological functions. The enhanced expression of myelin basic protein and Tuj1 highlighted the scaffolds' role in facilitating myelin and axonal regeneration. Moreover, they contributed to angiogenesis, a critical process for nutrient supply and tissue repair, by upregulating CD34 and vascular growth factor expression. Notably, graphene-based scaffolds exhibited dual regulation of Schwann cells and astroglia, positively influencing both central and peripheral nervous systems to promote neural repair. Despite these advancements, several challenges hinder clinical translation. The variability in biocompatibility results, stemming from differences in experimental models, presents a significant hurdle. Concerns about the long-term toxicity and limited biodegradability of graphene-based materials, especially at higher concentrations, also require deeper investigation. Additionally, understanding the interactions between graphene-based scaffolds and diverse cell types, alongside their effects on immune responses in large animal models, is crucial to ensure safety and effectiveness before advancing to human clinical trials. The graphene-based neural interface developed by INBRAIN Neuroelectronics represents one of the most advanced and successful examples of translating 2D material technologies from academic research into real-world medical applications [11]. By overcoming key challenges in scalability, industrial fabrication, regulatory approval and interdisciplinary collaboration, INBRAIN not only brought graphene-based devices closer to clinical use but also demonstrated a viable pathway for other emerging nanotechnologies. Their progress, culminating in FDA Breakthrough Device Designation and the launch of first-in-human clinical trials, serves as a model for how strategic partnerships, sustained funding and startup-driven innovation can bridge the critical 'lab-to-fab' gap in advanced medical technologies. Functionalization of 3D nanofibrous scaffolds made of decellularized ECM derived from porcine adipose tissue with polydopamine (PDA)-rGO enhanced its bioactivity and electrical conductivity, both very important for neural tissue engineering. Doping with PDA-rGO significantly boosted the performance of scaffolds towards neuronal differentiation, particularly in the 3D environment, which on its own created biomimetic environment that supported neural SCs adhesion, proliferation, migration and differentiation

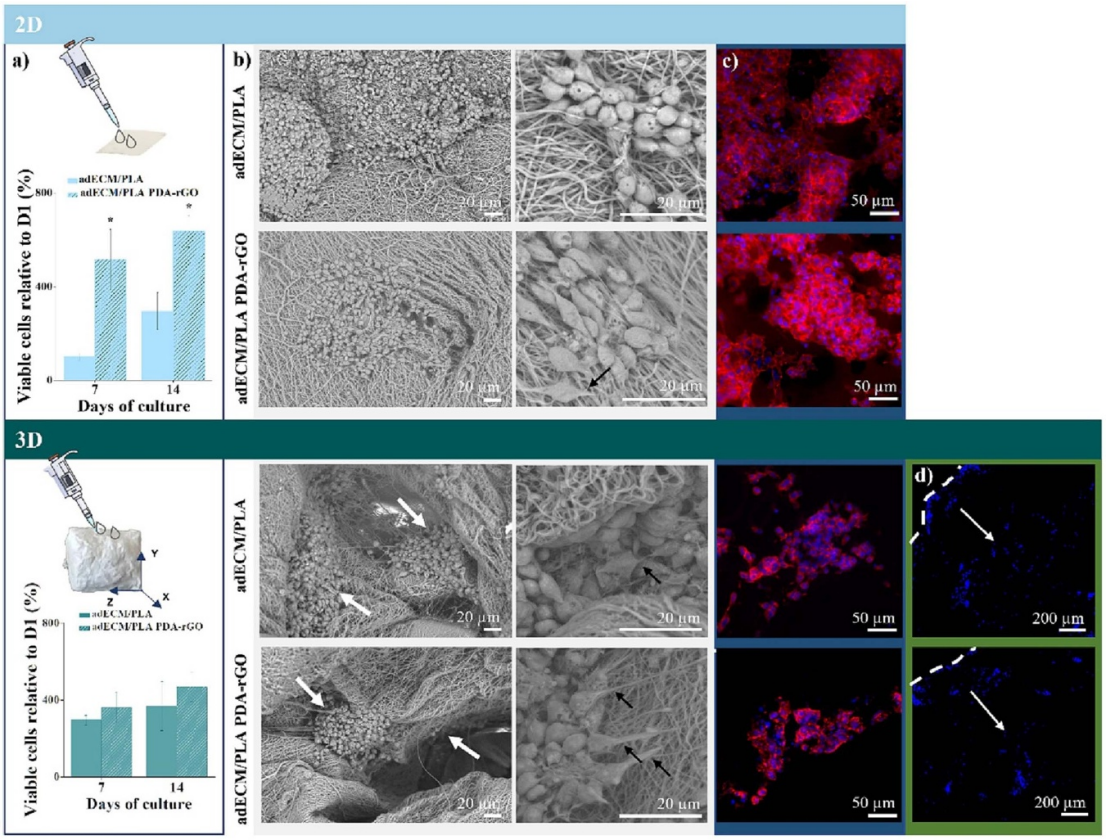

Figure 4. Proliferation and morphology of NSC-seeded bidimensional and three-dimensional platforms: (a) percentage of viable NSCs on the platforms relative to the adhered cells on day 1, after 7 and 14 d of culture and schematic illustrations of the seeding process in each platform; (b) SEM images of the NSCs-seeded platform after 7 d of culture, with white arrows highlighting the cellular clusters and black arrows pointing to the out-growing processes; (c) immunocytochemistry of actin filaments (phalloidin in red) and nuclei (DAPI in blue) of the NSC-seeded platform after 14 d of culture; (d) DAPI staining of the cross-sectioned NSC-seeded 3D platforms, with white arrows showing the cellular migration pathway. Reprinted from [48], Copyright (2023), with permission from Elsevier.

[48]. The scaffold also facilitated spontaneous differentiation, favoring a neuronal over an astrocytic lineage. In more detail, PDA-rGO in 3D platforms significantly enhanced neuronal differentiation, resulting in a 1.26-fold increase in Tuj1 levels and a 1.72-fold increase in MAP2a/b neuronal isoforms (see figure 4). Graphene, GO and rGO nanosheets, thanks to their large surface area, functionalized with molecules that enhance the ability to penetrate blood–brain barrier (BBB), can carry a variety of biomolecules, targeting the specific cell type or area in central nervous system. By serving as efficient drug delivery systems capable of crossing the BBB with ease, these nanosheets offer a promising solution to overcoming the challenges associated with drug delivery to the brain [49, 50]. The functionalization of rGO with polydopamine (PDA) has been shown to significantly influence SCs behavior, particularly by encouraging spontaneous differentiation toward the neuronal lineage [48]. This effect is observed in both 2D and 3D culture platforms, suggesting that PDA-rGO can serve as a powerful biointerface for neural tissue engineering. The gas foaming technique offers a simple yet effective method for generating 3D nanofibrous constructs with tunable physical properties. This approach allows the creation of biomaterial-based microenvironments that closely replicate native extracellular matrices, revealing biomaterial-induced cellular responses that may remain undetected in traditional 2D cultures. By incorporating PDA-rGO into gas-foamed 3D scaffolds, its potential as a neurogenic biomaterial can be assessed, revealing new possibilities for neural tissue engineering and regenerative medicine. The ability to fine-tune material properties using gas foaming further enhances its adaptability for various biomedical applications. Additionally, excellent electrical conductivity attributed to the structure of MoS_2 with unsaturated d-orbitals, and biocompatibility create nurturing microenvironment for neural SCs differentiation, allowing their attachment to porous architecture, efficient charge transport at the cell-membrane interface, proliferation and differentiation into neural cells [51]. This differentiation is marked by the increased expression of key neural markers such as Tuj1, GFAP, and MAP2 over extended culture

periods [52]. The porous nature enables stronger protein absorption, including growth factors like EGF and FGF, which further supports the maintenance of neural SCs stemness and promotes differentiation efficiency over time.

Its structure also provides excellent template for cell elongation, which is a preferred feature in neural tissue regeneration. Moreover, 3D cylindrical scaffolds made of MoS_2-PVDF hybrid films, with randomly assembled MoS_2 nanoflakes, showed potential for nerve regeneration encompassing flexibility, conductivity and compatibility, hence mimicking natural neural structures [51]. Significant regenerative potential through the light responsive properties of 2D materials with the focus on G and derivatives and TMDs lays within their capability to finely modulate cellular response. Excellent conductivity and photothermal capabilities stimulate cell growth, differentiation and tissue regeneration, particularly in neural and muscle tissues by non-genetic optical modulation. NIR light stimulation of MoS_2 nanosheets influenced more genes related to cell migration and wound healing in MSCs than nanosheets itself, as evidenced by transcriptome sequencing [53, 54].

BN nanosheets functionalized polycaprolactone channel scaffold was evaluated for neuronal repair through piezocatalytic stimulation [55]. This 3D scaffold, produced by layer-by-layer droplet spraying method, is highly elastic, hydrophilic and biocompatible [56]. After ultrasonic actuation, the scaffold generates bioelectrical signals that promote the secretion of neurotrophic factors, enhancing Schwann cell viability and modulate ROS levels to maintain metabolic balance. Schwann cell cultured on this scaffold showcased an increased expression of proliferative and neural markers (Ki67, Tuj1 and MBP), alongside reduced oxidative stress and elevated growth factor expression. *In vivo,* improved nerve regeneration, remyelination and functional recovery in a rat sciatic nerve defect model were observed. Higher nerve conduction velocities, enhanced axonal alignment and improved muscle reinnervation compared to control groups were noted as well as promoted angiogenesis and reduced amyotrophy. High biocompatibility of the scaffold played significant role all along.

3. 2D materials as humidity sensors

The increasing interest in wearable devices, namely, flexible and transparent sensors, has expanded the demand for novel materials [57]. Electronic devices that can be attached to the skin and that are able to continuously record vital signs are going to minimize both the size and the cost of healthcare monitoring. These types of devices require developing of a variety of noninvasive sensors for monitoring of human physiological biomarkers. For example, tracking the gas molecules that are transmitted from the body can play an important role in personalized medicine. The main requirements for these functional sensors is to be able to get comfortably attached on human skin and continuously and unobtrusively monitor human activities. Hence, this type needs to be conformable to the skin, and the substrate should not be an irritant. Some of the activities that should be uninterupptedly tracked are vital signs (respiration, pulse, blood pressure) and physiological activities (muscle movements, cognitive states). Furthermore, basic humidity sensors can have wide application in various fields outside of medical uses, such as environmental monitoring, agriculture, industrial production, process control and safety.

Some of the drawbacks of commercially available sensors is that they are mostly made of polymer films or porous ceramics, and are unable to operate at high humidity levels, have slow response time, high levels of hysteresis and a long-term drift. 2D layered materials have been extensively studied and shown great potential as resistive gas sensors due to their excellent electrical, physiochemical, and mechanical properties [58–60]. The need for these types of sensors is becoming highly important as the air pollution, caused by gases such as NO_2, SO_2, CO; VOCs and particulate matter, becomes ubiquitous. In this review, we focus on their emerging potential as humidity, human respiration and touch sensors. We firstly describe various mechanisms for humidity sensing from the aspect of sensor fabrication. In the next step, we assess the performance of different families of 2D materials, with the summary of relevant parameters.

3.1. Humidity sensing mechanisms

Humidity sensors can be fabricated through a variety of methods. While the majority of the commercially available sensors are capacitive-based, devices based on resistor/impedance response are becoming increasingly popular due to easier fabrication. In recent years, new operating mechanisms are emerging based on FET, QCM and fiber-optics. Here, we outline the most prominent sensing mechanisms and their advantages and disadvantages.

3.1.1. Capacitive

Commercially available humidity sensors are mostly based on the capacitive technique, where the dielectric constant of the active layer changes in response to humidity. The standard mechanism consists of parallel plate capacitors, where an intermediate moisture-sensitive dielectric layer is sandwiched between two metal electrodes. As the output, the change in capacitance is recorded, which occurs when the distance between the two electrodes changes (i.e. upon water molecule adsorption). The variations in capacitance also depend on the area of the electrodes and the dielectric constant of the intermediate material. The

straightforward assembly of parallel plate capacitors has led researchers to develop capacitive sensors using diverse materials, and to improve their flexibility and sensitivity. Nevertheless, capacitive sensors have several drawbacks, including hysteresis, stability at high temperatures and humidity levels, limited durability against certain organic vapors and their fabrication can be expensive.

The capacitance value is defined as:

$$C = \varepsilon A/d$$

where ε represents the dielectric constant, A the area of the capacitor, and d is the distance between the capacitor plates.

The response of the sensor is defined by the following formula:

$$\text{Response} = \frac{C - C_0}{C_0}\, x\, 100\%$$

where C_0 and C represent the capacitance measured under dry air and measured humidity, respectfully.

Sensitivity of the sensor is calculated using the equation

$$S = \frac{\Delta R}{R\Delta\%RH} X 100$$

where S is defined as the percent change in resistance divided by the percent change in relative humidity (RH), RH is defined as the ratio of 'water vapor present in a particular volume and at a particular temperature' to the 'maximum capacity of air to absorb the water molecule at the same volume and temperature'.

The response time is defined as the time required for reaching 90% of the total response value, while the recovery time is defined as the time required to return the response to 10% of the total response value.

The change in RH is detected as the change in voltage, as the conversion circuit (usually, a simple RC circuit) is transforming the change in the capacitance into change in voltage.

Capacitive-based humidity sensors have been reported on GO [61–65] and MoS_2 [66], which will be discussed in more detail in section 3.2. Figure 5 depicts two setups based on GO [61] and GO-PSS film [63].

3.1.2. Resistive

In contrast to capacitors, resistive humidity sensors have a simpler structure and are easier to integrate with CMOS technology. As a result, considerable research is focused on the development of resistive humidity sensors, which are expected to lower the cost per unit and offer improved long-term stability.

The sensing mechanism is based on recording the change in humidity, as the adsorbed water molecules affect the electronic density of states and the carrier concentration of the active material and change its conductivity.

The response is defined as:

$$\text{Response} = \frac{R - R_0}{R_0} x100\%,$$

where R_0 and R represent the resistance measured under dry air and measured humidity, respectfully.

A typical response of this type of setup, prepared on a hybrid composite of rGO and MoS_2 [67], is shown in figure 6.

3.1.3. Impendence

Sensor with impedance output is structurally similar to the resistive sensors, whereby they consist of three parts, a substrate, interdigital electrodes, and the sensing material. The output is highly dependent on the frequency and RH. Sensors show better performance at lower frequencies, as the impedance significantly increases with the decrease in both RH and frequency. In the typical setup, the output current is measured by applying a sinusoidal voltage to the electrodes, and the impedance is calculated as the voltage/current ratio. Some of the reported impedance-based sensors used GO [68], MoS_2 [69, 70], MXene [71], Al_2O_3 NTs [72] as the sensing material, and their performances will be discussed in detail in section 3.2. Two typical setups are depicted in figure 7.

3.1.4. Other sensing mechanisms

Other than the previously explained mechanisms, based on resistive or capacitive effects, new approaches have been proposed. Here, we discuss the most promising ones, which bring forth better integration into electronics, or miniaturize the size of the sensing device.

QCM

Quartz crystal microbalance is a technique capable of detecting mass change as small as the sub-nanogram, making it suitable for vapor phase sensors. A thin slice of quartz crystal is placed in a circuit, and with the applied voltage, alternating compression and stretching vibrations appear [73, 74]. The change in the resonant frequency can be detected, as the adsorbed water molecules change the mass of the crystal. The amount of the adsorbed water and the resonant frequency change are correlated, allowing for the calculation of the humidity level. This type of setup is shown in the left panel of figure 8.

Potentiometric

A self-powered potentiometric mechanism was reported [75]. The sensing mechanism was based on a sandwiched material structure, made of rGO/GO/-foamed metal (such as nickel, zinc, iron and copper), and it modulates the measured potential difference between the two electrodes by humidity

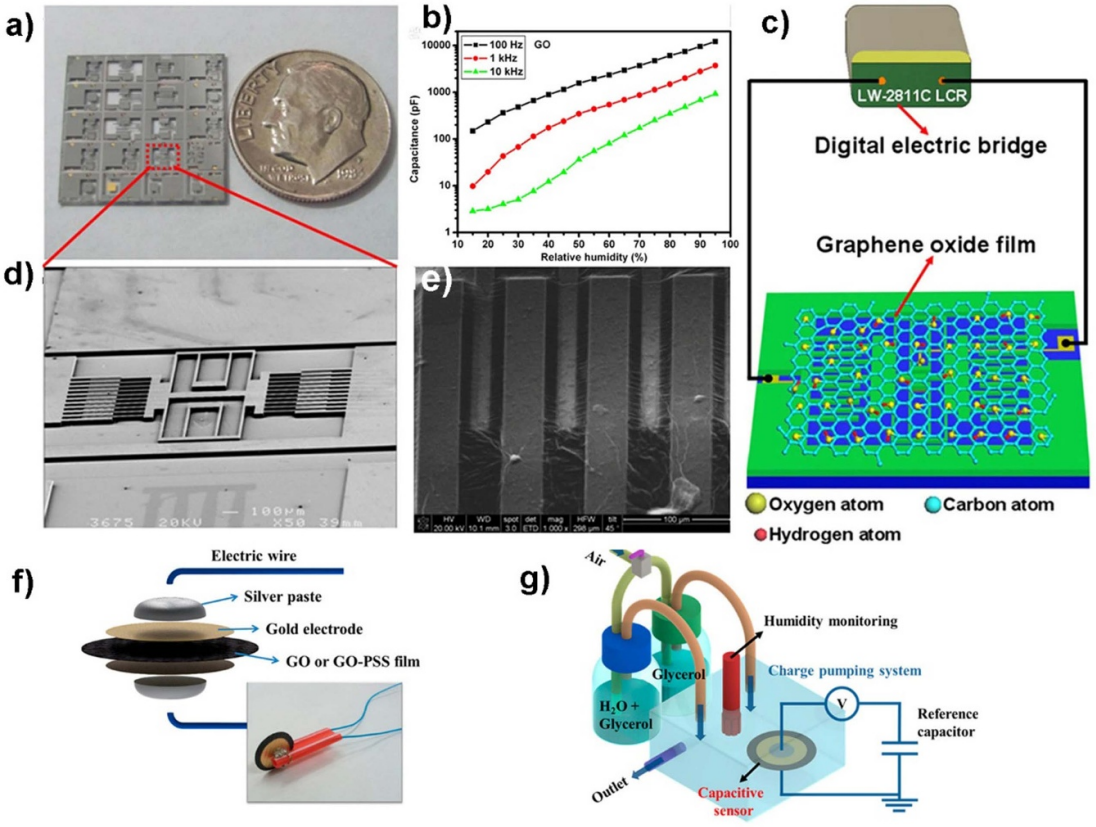

Figure 5. Capacitive-type humidity sensors based on (a)–(e) GO [61] and (f), (g) GO-PSS film [63]. (a) Digital photographs of the device, (b) SEM image of the area set off by a red dashed line, (c) output capacitances of sensors as a function of RH, (d) SEM image of interdigitated electrodes covered with GO films, (e) schematic diagram of the humidity testing system of GO as a humidity sensing material between the two sets of interdigitated electrodes. (a)–(e) Reproduced from [61], with permission from Springer Nature. (f) Sensor based on the GO and GO-PSS dielectric films. An optical image of the fabricated sensor is shown in the inset. (g) Schematic diagram of the RH controlled-environment chamber and charge pumping system. Reprinted with permission from [63]. Copyright (2014) American Chemical Society.

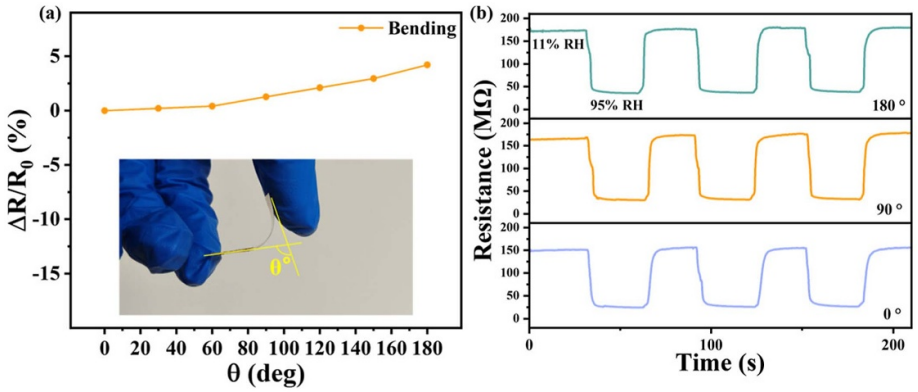

Figure 6. Resistance response of a device based on rGO and MoS_2 as it was gradually bended in the atmospheric environment. (b) Humidity experiments of a device with the relative humidity change between 11% RH and 95% RH as it was bended with different bending angles (0, 90, and 180°). Reprinted with permission from [67]. Copyright (2024) American Chemical Society.

stimulation. While the resistive or capacitive devices are difficult to miniaturize because they require an external power supply, potentiometric humidity-transduction method is able to detect both steady and rapid humidity response of multiple cycles with high response value and short response/recovery time (RRT). The external humidity stimuli can regulate the hydration across GO, as a solid electrolyte, and bring about a change in the output voltage measured between the two electrodes. The sensor showed high stability, high RRT and was able to monitor both the static and dynamic humidity stimulation.

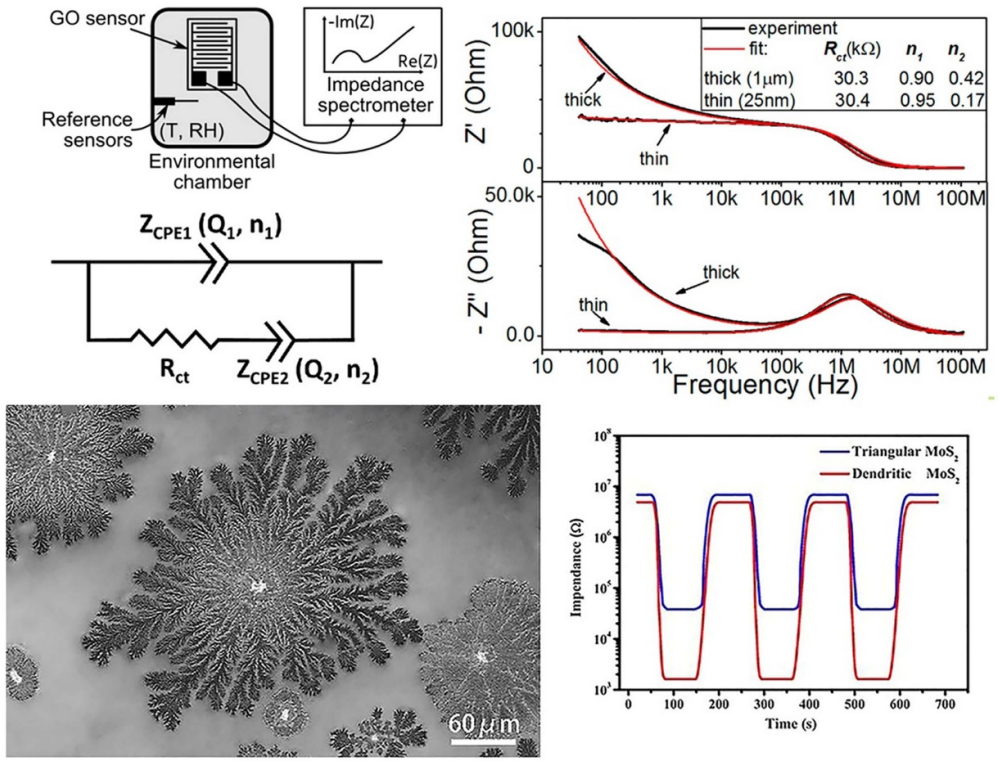

Figure 7. Impendence-based humidity sensors. Top panel: diagram of the experimental setup and fitting of the impedance spectrum, by using the displayed equivalent circuit, for two different GO film thickness values and the conductance response of an ultrathin GO film to RH variation. Reprinted with permission from [68]. Copyright (Year) American Chemical Society. Bottom panel: SEM images of dendritic MoS_2 and impedance vs RH curves of dendritic MoS_2 and triangular MoS_2 at 100 Hz. Reprinted from [70], Copyright (2020), with permission from Elsevier.

Fiber optics

Sensors based on fiber optics are helpful for overcoming the drawbacks of electrical sensors, as they have fast response, high accuracy and long service life. They are easy to fabricate and are compatible with pre-established fiber optic systems. The sensing mechanism is based on the change in the light transmission. Namely, the water molecules adsorbed by the high refractive index (RI) coating result in a difference in the reference optical signal and the detected signal. This change can be used to calculate the humidity. For example, by overlaying WS_2 on side of a polished fiber, a first all-fiber-optics humidity sensor was developed, with rather fast RRT (1 s/5 s) [76]. This setup holds a lot of promise, and by using some other high RI materials, such as MoS_2, or the combination of materials, RRT can potentially be improved.

FET

Field effect transistor-based sensors have a standard setup of a source, drain, gate and channel materials. Channel material is the active sensing material and it bridges the source and the drain. The sensing materials absorbs or releases water, affecting the charge distribution between the layer and the gate. Graphene is not a good candidate for FET-based sensors due to low on/off ratio and zero bandgap, therefore, these types of devices are reported on MoS_2 [69] and metallic nanowires (NWs) [77].

3.2. Sensing performance of 2D materials

Here, we assess the performance of humidity sensors for a variety of 2D materials. The summary of critical parameters, such as type of the device, material, mechanical status (whether it is rigid, flexible or stretchable), the measured humidity range, the RRT and the response/sensitivity of the device are presented in table 2. *NA* stands for parameters which were not reported (and cannot be deduced) in the paper, in the units typical for that specific measurement setup.

3.2.1. Graphene, GO and rGO

Graphene, GO and rGO [61, 62, 64, 68] were all studied as sensing materials, and their performances will be discussed here in detail.

As previously mentioned, single layer graphene has high electrical conductivity ascribed to the p-orbital electrons, which form π-bonds with neighboring atoms. On the other hand, delocalized π-electrons are sensitive to the modifications of their immediate environment, making them suitable for sensing [99]. Nevertheless, humidity sensors based on graphene alone have shown limited range and/or response times [100]. Some of these drawbacks can

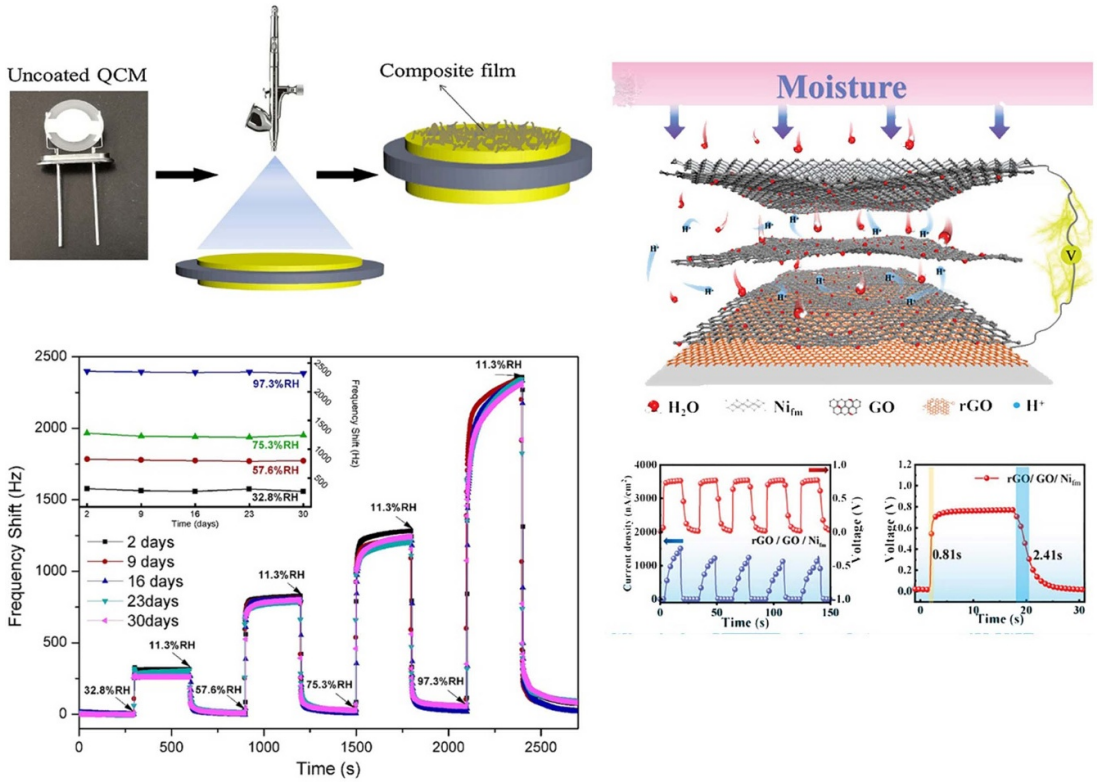

Figure 8. Left panel: QCM-based sensor. Top: fabrication illustration. Reprinted from [73], Copyright (2018), with permission from Elsevier. Bottom: dynamic frequency shift of QCM sensors, inset are response values versus RH. Reprinted from [74], Copyright (2016), with permission from Elsevier. Right panel: potentiometric humidity sensor design: schematic illustration of the humidity response mechanism; response/recovery curve of open circuit voltage (V_{oc}) and short current density (I_{sc}) of rGO/GO/Ni_{fm} sensor and the response/ recovery time of rGO/GO/Nifm sensor. [75] John Wiley & Sons. © 2021 Wiley-VCH GmbH.

be overcome by using CVD graphene. For example, graphene deposited on a SiO_2 layer on a Si wafer, was prepared as a resistive humidity sensor and showed response time comparable to GO [79]. As there has been extensive work done on graphene, we will focus more on GO and rGO.

GO film is a laminated material formed from oxygenated graphene platelets. It is a good candidate for humidity-response platforms, as it is a low-cost, easily synthesized material. It possesses a large specific surface area, which can highly improve the number of exposed atoms at the edges that can act as water molecule absorbers. It also contains diverse oxygen-containing groups on a basal plane, and carboxylic acid groups at the edges, which can increase hydrophilicity [75]. These characteristics allow GO to be utilized as humidity sensing material, as the layered and interlocked structure of GO films effectively undergoes the permeation of water molecules into the film under humid conditions [101]. Nanoscale capillaries between individual GO platelets facilitate low-friction water molecule flow on the surface, making the permeation process both rapid and reversible [102]. As a result, the interlayer distance between GO platelets increases with increasing RH, making it possible to monitor the humidity in the environment.

The sensing mechanism based on resistivity has been developed by measuring the electrical conductance changes in the GO films upon the exposure to a humid environment [103]. Namely, electrical interactions between water molecules and GO platelets cause electrical perturbations in the GO films that can be monitored in real-time. The water molecules that are hydrogen-bonded to the oxygen groups on the GO surface easily lose a degree of rotational freedom because of the strong interactions in the layered and interlocked structure between the platelets. As a result of the confined water intercalation through exposure to humidity, there is an increase in dielectric strength and a decrease in the electrical conductivity of GO films. A capacitive-type humidity sensor was prepared, reporting high sensitivity, explained as a result of violent oxidation and a creation of large density of sulfur vacancies and hydrophilic (carboxyl, hydroxyl) functional groups [61]. Through previously mentioned basal plane and edges of GO, composed of distributed oxygen groups, the hydrophilicity is improved. Another GO humidity sensor was prepared on chemically exfoliated

Table 2. Summary of the device performance based on sensing material, mechanical status, testing RH range, response or sensitivity and response/recovery time. NA stands for non-applicable, i.e. this parameter was not evaluated.

Device	Material	Mechanical status	RH range (%)	Response/sensitivity	Response/recovery time (s)
Capacitor	GO [61]	Rigid	15–95	37 800% at 1 kHz	10.5/41
	GO/PDDA [62]	Flexible	11–97	1552 pF/% RH	108/94
	GO/PSS [63]	Flexible	20–80	NA	60/50
	GO-Au [64]	Rigid	11–97	25 809 pF/% RH	8/12
	GO [65]	Flexible	10–90	3215.25 pF/%RH	15.8/NA
	MoS_2 (liquid exf) [66]	Rigid	11–96	43 684%	30/40
Resistor	rGO [78]	Flexible	10–95	100	50/3
	Graphene [79]	Rigid	1–96	S%: 0.31 (ΔR/R/%RH)	0.6/0.4
	GO [80]	Flexible	30–95	S%: 7.9	100/NA
	rGO/PU [2]	Stretchable	10–70	$\Delta R/R_0$ 4.63 at RH = 35%)	3.5/7
	GO [81]	Rigid	8–95	124%	3/7.7
	r-CMGO [82]	Rigid	0–100	0.33%RH − 1	0.025/0.127
	rGO [83]	Rigid	11–97	NA	15/28
	MoS_2/GO [84]	Rigid	25–85	IH/IB = 1600	43/37
	rGO/MoS_2 [85]	Rigid	5–85	2494.25	6/31
	rGo/MoS_2 /PI [67]	Flexible	11–95	96.7%	0.65 s/14.4
	MoS_2 (nanosheets) [86]	Rigid	10–60	NA	9/17
	MoS_2/Si NW [87]	Rigid	11–95	392%	26/15
	MoS_2/PEO [88]	Flexible	0–80	$\sim$0.7 $\Omega\,^{\circ}C^{-1}$	0.6/0.3
	MoS_2 NTs [89]	Rigid	20–85	668	0,5/0,8
	MoS_2@$MoSe_2$ flowers [90]	Rigid	H_2O conc 25–12 000 ppm	NA	30/33
	WS_2 NPs [91]	Rigid	11–97	469%	12/13
	WS_2 nanosheets [92]	Rigid	8–85	IH/IB = 1300 at 85% RH	140/30
	MoS_2 NPs-plasma [93]	Rigid	20–95	NA	0.5/0.8
	SnS_2 nanoflakes [94]	Rigid	11–97	−11 300%	85/6
	SnO_2 film [95]	Flexible	15–70		
	CeO_2 NW [96]	Rigid	15–97	*R*air/*R*RH = 6.2	3/3
	ZnO NW [97]	Rigid	17–60	4000 for 50% RH	60/3
	MXene/TPU	Flexible	11–94		12/30
Impendance	GO [68]	Flexible	35–80	NA	0.03/0.09
	MoS_2 dendrites [70]	Rigid	10–95	413 S = Im (11%)/Im (95%)]	17/24
	MoS_2—spiropyran [69]	Rigid	10–75	1.0% · (%) RH − 1	NA
	MXene/GO/COC [71]	Flexible	6–97	182 * 10^6/%RH at 1 Hz	0.8/0.9 s
	TiO_2 NW [98]	Rigid	11–95	3000%	3/7
	Al_2O_3 NT [72]	Rigid	11–95	10 000%	10/20
QCM	GO/PEI [74]	Rigid	11.3–97.3	27.3 Hz/%RH	53/18
	GO/SnO_2/PINI [73]	Rigid	0–97	29.1 Hz/%RH	7/2
Potentiometric	GO [75]	Rigid	20–90	5–20 mV/%RH	0.8/2.4
Fiber optics	WS_2 [76]	Rigid	33–85	0.1213 dB/%RH	1/5
FET	SnO_2 NW [77]	Rigid	NA	NA	120/20

large-area thin films [80]. While easier to scale-up, these films showed a slow response time of 100 s.

In another approach, a GO-based single-layered sensor chip with multiple sensing capabilities was prepared [81]. It showed potential to operate as a microheater, temperature sensor and a flow sensor. This device was fabricated on two sides of the Si wafer. On one side of the chip, a GO-based humidity sensor is fabricated, offering ultrahigh sensitivity of 124/% RH, rapid RRT, and a wide detection range (8%–95% RH). Additionally, the effect of temperature on the humidity sensing properties of GO is demonstrated using the microheater platform. On the other side of the chip, serpentine Pt micropatterns serve

as high-performance temperature and flow sensors in cold and heated states, respectively, when connected to the appropriate circuits. Low and high voltages are applied to the Pt microlines for temperature and flow sensing, respectively, generating negligible and significant Joule heating effects. As a result, the Pt micropatterns enable the realization of three distinct functionalities within a single device. The humidity was tested from 8% to 95%, with fast RRT of 3 s/7.7 s. Another technique used to increase the active surface area is to combine GO with metal NPs. For example, Ag NPs were added to GO in different concentrations, in order to improve the humidity sensitivity of capacitive-type sensors [64]. The sensing properties were tested in a 11%–97% RH range at room temperature. The best performance was achieved by the GO/Ag (2 wt%) composite-based sensors. Addition of Ag NPs increases the large specific surface area and hydrophilicity by adding the wrinkles. Beyond 2%, the initial resistance of the composites becomes too small to be dielectric, and the performance of the sensor deteriorates.

Nevertheless, sensors based on natural GO have limited sensitivity at low humidity levels. The material is also electrically insulating, but its conductivity could be partially restored if certain reduction processes are performed to remove oxygen groups. Therefore, rGO can sustain both the conductivity and the chemically active defect sites. One drawback is its relatively low surface area, which significantly hinders the sensing capabilities. Therefore, it is highly desired to prepare rGO as hierarchical nanostructures. Such a sensor was developed, whereby two-beam-laser interference was used to control the content of graphene functional groups [78]. With this approach, conductivity could be partially restored, leading to tuning of RRT due to the interaction between the water molecules and oxygen functional groups.

rGO was also prepared as a humidity sensor via modified Hummers' method, and showed faster RRT (15 s/28 s) than pure GO (18 s/31 s) [83].

Using a simple chemical modification of rGO with hydrophilic moieties can improve the sensing performance significantly. Another drawback of using rGO as a humidity sensor is the hydrophobic nature, as the reduction of GO removes the oxygen-containing functional groups. It was reported that, by using triethylene glycol chains, rGO resistive-based sensor increased the sensitivity by 31%, with ultrafast response (25 ms) and recovery (127 ms) times [82]. By using chemical functionalization of GO with carefully designed molecules allows for achieving optimal performance in humidity sensing while ensuring high selectivity to water molecules. Similar functionalization of GO and other 2D materials with specific receptors for the desired analyte, strategically selected from the well-established library of supramolecular chemistry, will enable the creation of high-performance chemical sensors for a wide range of analytes.

3.2.2. MS_2

In the covalently-bonded S–M–S (M is a transition metal such as Mo, W, Sn), MS_2-layers are bound together by van der Waals interactions. The atoms of each individual layer can be classified into basal plane sites and edge sites. The basal plane is terminated by sulfur atoms with lone-pair electrons and no dangling bonds, making it inactive. In contrast, the edge sites, where either transition metal or sulfur atoms lack coordination bonds, tend to be more active. As the analogue of graphene, semiconducting MS_2 materials, together with lower background carrier densities, are expected to display a comparative or preferable sensing performance. Furthermore, they are suited to be a good sensing platform, as this family of materials has excellent thermal stability, ideal bandgaps, very high mobility and strong electron–hole confinement. One of the first successful humidity sensors based on MoS_2 was reported in 2012, on a two- and five-layer resistor-type device, but this early work shows slow recovery and response times [104].

One of the drawbacks of the devices based on single-layer films is that they suffer from an unstable current response and are not suitable for scale-up [105]. One of the solutions is fabrication of devices based on liquid-phase exfoliated nanosheets [66]. This method of exfoliation increases the molecular adsorption area, due to the presence of dangling bonds at the edge sites and defects and vacancies. The resulting sensor showed RRT of 30/40 s. Moreover, MoS_2-based sensors show lower hysteresis than GO-based sensors, which have strong interaction between GO oxygen functionalities and the physisorbed water molecules [82]. Furthermore, few-layer nanosheets have a superior long-term stability, and they do not need to be functionalized with NPs or polymers to improve the slow recovery. Another resistive device based on a exfoliated thin film of MoS_2 was prepared by drop-casting and tested in the RH range of 0%–60% [86]. This sensor showed fast RRT of 9 s/17 s, surpassing that of bulk MoS_2. This effect can be explained by the increased surface area of the nanosheets after exfoliation, leading to more water molecules absorption sites. When MoS_2 is exfoliated into few-layer nanosheets, it exposes a significant number of low-coordination step edges, kinks, and corner atoms. These exposed edge sites play a crucial role in the material's gas sensing behavior. Another large-area few-layer MoS_2 film heterojunction was prepared with Si NWs array [87]. While the contact area of MoS_2/bulk Si is not large enough to be used as a detector, resulting in poor device performances, using NWs can increase the specific surface area, improving the sensitivity and response speed.

This sensor showed high sensitivity with the RRT of 22 s/12 s.

Although functionalization is not required for improving the stability, this process can be used to introduce other mechanisms, such as light switching. By interfacing them with organic photocromatic molecules such as spiropyran (SP), electronic characteristic of 2D materials can be modulated [69]. SP-functionalized MoS_2 light-switchable bi-functional field-effect transistors were reported [106]. SP exhibits reversible photo-isomerization from neutral (SP) form and a zwitterionic merocynine (MC) form through UV light. Owing to this effect, the functionalization of 2D surfaces with SP molecules represents a useful approach to confer to them a reversible light-controlled wettability. It was demonstrated that decorating mechanically exfoliated MoS_2 with solution-processed SP, functionalized with either ethylene glycol chains (EGO-SP) or alkyl chains (C13-SP), provides an effective approach to modulate the sensitivity of FETs to humidity changes. This is achieved by using a subtle, non-dynamic control over the interaction with environmental water molecules. The light-induced photo-switching triggers a wettability change of the SP/MoS_2 interface, which, in turn, worsens the optoelectronic properties of the MoS_2 semiconductor due to water's known role as an electron trap in MoS_2. The reversible behavior of water adsorption on the MoS_2 surface was evaluated through repeated exposure of the device to humid and dry air. It was observed that the MoS_2 device's initial performance could be partially restored after 1 h of flushing with a gentle stream of N_2 to remove the water.

While the pure MoS_2 humidity sensors suffer from low sensitivity at room temperature, coating them with metal NPs can increase their performance, but it also increases the cost. Combining GO with MoS_2 flakes to prepare a nanocomposite showed significant improvement as a chemoresistive humidity sensor [84, 85]. In the nanocomposite, water molecules attach to defect sites found in both the MoS_2 and GO layers. Additionally, the functional groups on the GO layer facilitate the adsorption of water molecules. Due to the large surface area of both MoS_2 nanoflakes and GO nanosheets, the amount of adsorbed water is significant, which in turn increases the density of charge carriers. The high response of the RGMS humidity sensor was attributed to the p–n heterojunction formed by the p-type rGO and n-type MoS_2 and the effect of the oxygen functional groups remaining on the surface of rGO.

MoS_2 can be prepared in other morphologies in order to increase the surface area. For example, MoS_2 nanoflowers were decorated with Au NPs in order to enhance electrical conductivity of the humidity sensor [107]. The prepared solution was drop casted on an electrode and mounted on a cotton mask so that it sits between the nose and the mouth and detects breathing. The sensor showed promising results with RRT of around 100 s. $MoSe_2$@MoS_2 nanoflowers were synthesized and tested as humidity sensors with a unique 3D interface structure [90]. The direct growth of MoS_2 on $MoSe_2$ nanosheets spontaneously forms a high number of n–n heterojunctions enabling more sensitive adjustment of resistivity by influencing interface electron transfer efficiency. By finding an optimal ratio of these two moieties, a sensor with improved sensitivity and response times with respect to single-phase sensors was achieved. The fastest times were 40 s/33 s for a 50:50 ratio, and the sensitivity increases almost 10 times than that of the single-phase material. Few-layer dendrites of MoS_2 were prepared via CVD method and deposited on Si/SiO_2 substrate. This fractal configuration increases the humidity sensing performance due to the increase in structural complexity and edge active sites [70]. The dendritic MoS_2 has a lower impedance and a higher rate of change for the same response time compared to the triangular MoS_2. The RRTs were 11 s/17 s and 17/24 s, respectively. Under high RH conditions, free water can penetrate the interlayer of dendritic MoS_2 nanomaterials, enhancing the dielectric constant and sensor response. The abundance of edge active sites contributes to its high conductivity and faster charge transfer, significantly improving its humidity sensing properties.

Another approach to modify and improve sensor parameters is by plasma irradiation. MoS_2 NPs were exposed to O_2 plasma, which increased the total pore volume and the specific surface area, while shifting the pore size distribution towards lower values [93]. O_2 plasma can have several effects on 1T/2H NPs. It can create defects in the crystal structure; it can act as the etching medium and remove the excessive sulfur. It is also possible that the heat generated by plasma can change the phase structure, and increase surface roughness due to formation of MoO_3. Response/recovery times for non-treated MoS_2 were 76 s/382 s, while the treated showed an increase in response time and decrease in recovery time. The decrease of the pore size slows down the diffusion of water to the pore surfaces to decrease the response time.

WS_2 was tested as humidity sensors both in the shape of nanosheets and NPs. WS_2 NPs, in the size range of 25–40 nm, were deposited on a quartz wafer [91]. The fast recovery time (13 s) is attributed to the fast desorption process of H_2O molecules from the WS_2 NP, and the slow response (12 s) is due to hydrophilic surface of the NP resulting in slow adsorption of H2O molecules on the surface. 2D-WS_2 nanosheets were prepared via exfoliation and drop-casted on a commercial alumina substrate with Ag electrodes [92]. This resistive sensor showed RRT during a pulse between 8 and 85 RH % of 140 s and 30 s. While the reported times are not fast, the sensor showed high

stability, as it had a nearly constant response over many weeks. An all-fiber-optics sensor based on WS_2 showed rather fast RRT (1 s/5 s) [76].

SnS_2 is another layered material, where tin cations (filling the octahedral sites of the alternating layers) and sulfide anions form hexagonal structures, and it is gaining interest due to its stability. SnS_2 nanoflakes, prepared by an economically viable hydrothermal synthesis method, were tested as humidity sensors [94]. This sensor showed promising recovery time of 6 s, with the longer response time of 85 s. The response of the sensor device is most likely constrained by the strong adsorption and desorption of analyte molecules at room temperature. The thermodynamic adsorption of analyte molecules may not be highly favorable during the response time, and during the recovery phase, analyte molecules easily desorb due to their low absorption energy. As a result, the response time is significantly longer than the recovery time.

3.2.3. Flexible sensors

In order to prepare flexible sensors, TMDC materials can be introduced into flexible substrates. Given the need for permeability, biocompatibility, and comfort in wearable devices, a variety of porous materials can be utilized as flexible substrates, with the polymers being the most popular. When the nanomaterials are added to a polymer matrix to prepare a composite, unique mechanical, thermal and spectroscopic properties can be achieved that would be otherwise infeasible with the individual materials. The nanomaterials add to the improvement of the overall strength and stiffness, making them the load-bearing component, while the polymer matrix uniformly transfers the applied force to the nanomaterial, serving as a load distributor. The parameters that determine the performance of such composite are the individual properties of the constituents, their weight ratio, and the geometry and the orientation of the nanomaterial in the composite. They can improve stiffness, toughness, structural and thermal stability and tensile strength. The potential use of silicon-based nanocomposites as flexible and stretchable sensors is opening up the search for the best filler for different applications, such as motion detection, structural health monitoring, artificial electronic skin, nanosensors [108, 109]. As they can have high stretchability and sensitivity, simple manufacturing process and fast response, they can be added to wearable devices or attached directly to the skin. Nanomaterials have been shown to be superior fillers to the conventional metals and semiconductors that are limited due to their poor stretchability, brittleness and dispersion difficulties. Variety of novel nanomaterials, such as NWs [110], graphene [111–113] and metal oxides [108], have been successfully incorporated into elastomers. These fillers can be further modified to enhance their integration with polymeric matrices and substrates and to tailor the sensing efficiency of the overall nanocomposite material.

A humidity sensor prepared from intrinsically stretchable components, instead of a combination of rigid and flexible materials, should be preferred. One of the first transparent and stretchable humidity sensors was reported on a rGO/PU (polyurethane) device [2]. This resistor-based sensor has a faster RRT than previously reported devices based on graphene and GO. It can detect the humidity of the human breath, remains stable up to a strain of 60% and after 10 000 stretching cycles at 40% strain. In other work, GO/PEI (Poly(ethyleneimine)) was sprayed on a QCM for humidity detection. This sensor exhibited high sensitivity, good RRT (53/18 s), negligible hysteresis and good repeatability [74]. QCM method was also used on a GO/SnO_2/PANI nanocomposite [73]. This composite has higher surface area, accessible pore volume and pore size distribution, as well as a smaller water contact angle than the separate GO/PANI and SnO_2/PANI composites. The sensing mechanism was analyzed using the Langmuir adsorption isotherm model. Water molecules are adsorbed on the GO/SnO_2/PANI nanostructure through the hydroxyl, carboxyl and epoxy functional groups attached on the GO nanosheets, the amino groups on PANI nanofibers, as well as surface vacancies and defects on SnO_2 NPs. The water molecules were firstly chemisorbed on the coated film at low RH, followed by physisorption by double hydrogen bonding. At high RH, the first-layer water molecules were physisorbed through the action of double hydrogen bonding. The resulting sensor has a rather short RRT (7 s/2 s), with high stability, making this sensing mechanism promising for future applications.

Using hydrophilic polymer can improve the characteristics of GO-based sensors. PSS (poly (sodium 4-styrenesulfonate)) was added as an intercalant between individual GO platelets to enhance the water permeation characteristics [63]. The capacitive-type humidity sensor fabricated by forming metal electrodes on the film was equipped into the charge pumping system, which can produce voltage outputs as a response to humidity sensing. Compared to the pure GO sensor, GO-PSS films showed a 3 times faster response to humidity and 5 times higher voltage output. In comparison with covalent bonding in GO and RGO, non-covalent methods could offer the π bonding on graphene basal plane while retaining graphene unique electronic properties without necessarily making use of harsh chemicals. One of the approaches to non-covalently functionalize graphene was to coat it with a thin layer of hydrophilic polymer. Trough functionalization with PEI (polyethylenimine), an amine-rich polymer, the electron transfer from amine groups to graphene improved the humidity sensing performance [114]. GO/PDDA multilayer film was fabricated on a polyimide substrate using

layer-by-layer self-assembly method and tested as a capacitive humidity sensor [62]. This sensor showed high sensitivity in the 11%–97% range, as well as a fast RRTs.

MoS_2 flake suspended in PEO were prepared as an active layer of a resistive temperature and humidity sensor with RRT of 0.6 s/0.3 s [88]. Furthermore, compared to the bulk MoS_2, MoS_2 NPs are more promising for improving the adsorption performance of water molecules/humidity because they have a high specific surface area, which is beneficial for enhancing the number of water molecules attached on the surface of MoS_2. A fully-flexible humidity sensor was prepared based on a hybrid composite of rGO and MoS_2 with high responsivity and fast response times [67]. rGO was chemically reduced in an environmentally friendly manner, mixed with MoS_2 via ultrasonic dispersion and the resulting GO/MoS_2 dispersion was drop-casted onto a PI substrate with interdigitated electrodes. The resulting flexible humidity sensor demonstrated a responsivity of 96.7% within the RH range of 11% RH–98% RH, along with fast RRT of 0.65 s and 14.4 s, respectively.

3.2.4. MXenes

MXenes, made from thin layers of transition metal carbides, nitrides, or carbonitrides, feature alternating metal and carbon layers. To reduce or control their conductivity for humidity-sensing applications, they can be functionalized or mixed with oxides, polyelectrolytes, and polymers. Sensing mechanism of MXenes is based on the abundance of hydrophilic active sites, such as –OH and –O terminated groups for water adsorption and intercalation [115]. They are great candidates for resistive sensing, as the intercalation of water molecules within the interlayer of MXene leads to an increase of resistance. Nevertheless, the incorporation of MXenes into flexible polymers remains a challenge, as the weak affinity between MXene and polymer fibers because the hydrophilic groups of MXene is incompatible to hydrophobic nature of polymers. It usually results in the exfoliation of sensing materials during the deformation process, restricting the stability of humidity sensors. One approach to solving this issue is coating MXenes with TPU electrospun nanofibers [115]. This sensor showed RRT of 12 s/30 s, respectively, with good stability.

Using GO as the sensing layer and MXenes as the electrodes in a humidity-sensing device offers numerous advantages. While GO exhibits a strong affinity for water molecules, MXenes, known for their excellent electrical conductivity, facilitate reliable measurement of the resistance changes in the GO layer, resulting in a more sensitive humidity sensor [71]. Furthermore, GO's highly interconnected 2D layered structure facilitates rapid diffusion of water molecules, resulting in fast response times. Its compatibility with TMNSs and flexible substrates makes it ideal for the development of flexible humidity sensors, which are well-suited for applications involving bending, molding, and mechanical stress. This type of a capacitive sensor exhibited a large response range of 6%–97%, with ultrahigh RRT of 0.8 s/0.9 s.

3.2.5. Metal oxides

Other promising humidity sensing materials are metal–oxide NWs and nanotubes [72, 77, 96–98]. While the conventional metal oxide-based sensors usually require high annealing temperatures (larger than 200 °C), NTs and NWs have many characteristic optimal for sensing, such as larger surface-to-volume ratio, higher surface activity, and better absorption performance. The tube-like nanostructures offer an increased number of efficient adsorption sites for water vapor, resulting in high surface charge densities that promote physisorption processes, thereby enhancing the sensor's sensitivity at low humidity levels. Amorphous Al_2O_3 NTs impedance-based humidity sensors were prepared, and showed promising RRT of 10 s/20 s [72]. CeO_2 NWs humidity sensors was reported, with the ion-type conductivity as the sensing mechanism [96]. They have a humidity-independent RRT of 3 s/3 s. LiCl-doped TiO_2 nanofibers [98] humidity sensors showed high RRT of 3 s and 7 s, with stability of one month with almost no changes in the impendences. Due to the 1D structure of the fibers, rapid mass transfer of water molecules to and from the interaction region is promoted, while also enhancing the rate at which charge carriers pass the barriers along the wires. Additionally, compared to 2D nanoscale films, the interfacial area between the active sensing region of the nanofibers and the underlying substrate is significantly reduced. These advantages result in a substantial improvement in the sensing signal and stability.

SnO_2 was used as a sensing layer and it was annealed using NIR laser, with low annealing temperature of 41 °C [95]. They were deposited on soft plastic wrap substrates. This ultra flexible SnO_2-based sensor can detect very small incremental changes (0.1%–2.2%) of RH in air, with RRT of 90 s/150 s. A single-NW SnO_2 humidity sensor was prepared as FET and tested as a humidity sensor for RH between 30% and 85% [77]. These NWs possess a large number of oxygen vacancies in the crystal; therefore, the surface is very sensitive to oxygen and water vapor in air. The RRTs were 20 s/60 s, faster than that of flat SnO_2. Additionally, when the sensor was kept in the moisture for about 1 h, the current still recovered to the original value, indicating that the interaction between water vapor and the surface of the NW should be dominated by physisorption, while chemisorption plays a minor role. A single ZnO NWs was deposited between gold electrodes and

placed into a chamber with humidified air [97]. These devices shows exponential change in the resistance of more than five orders of magnitude in response to a change of RH from a dry air to 60% RH air at room temperature. This is a result of a subthreshold carrier modulation in the NW core, high surface-to-volume ratio of the NW and complete exposure of the NW surface to air, due to the free standing structure. These sensors demonstrate stable behavior, reproducible switching response, with RRTs of 60 s/3 s time in response to 30% RH pulses between dry air flushes and pronounced sensitivity at elevated temperatures.

4. Human breath and touch monitoring

Respiration is one of the key human vital signs that reflects the state of the respiratory system and overall health. By monitoring respiration, health can be assessed through factors such as respiratory rate, depth, pattern, and oxygen saturation. In healthy adults, the normal respiratory rate typically ranges from 12 to 20 breaths per minute, while children tend to have a slightly higher rate. Abnormal rates can signal health issues such as anxiety, hypoxia, fever and other conditions, whereas slow breathing can be indicative of medication overdose or neurological disorders. The breathing pattern shows the regularity and rhythm of breathing. However, traditional respiratory monitoring methods often cannot provide real-time, synchronized, and comprehensive measurements. Typically, real-time monitoring requires wearing medical respiratory equipment, which can significantly interfere with normal activities. Therefore, the development of flexible respiratory monitoring e-skins is a crucial advancement in healthcare. Those novel respiratory sensors are designed to monitor human breath non-invasively by detecting, measuring and interpreting respiratory data in real-time. Some of the parameters they should track are respiratory rate and volume, and the composition of the exhaled gas. These parameters can be further used to diagnose respiratory disorders, and guide the physical activity after the recovery. For example, such wearable sensors were tested for early diagnosis of Covid-19, through non-invasive monitoring of the respiratory behavior, body temperature and blood oxygen level [116]. Graphene FETs were also able to detect SARS-CoV-2 spike protein [117]. This method of monitoring can be particularly useful for people outside of hospital settings. Specifically, humidity sensors can effectively differentiate the inhalation and exhalation phases, as well as the depth of each respiratory cycle, by detecting changes in RH during the inhale and exhale processes. Therefore, the sensor should be placed near the nostril or mouth, realizing contactless measurement. Additionally, respiratory monitoring based on RH in the airflow is minimally influenced by environmental factors such as temperature, noise, and others, ensuring reliable data. The breathing process consists of two periodic stages: inhaling air that contains O_2 into the lungs and exhaling CO_2 through the nose or mouth. The complete cycle, from inhalation to exhalation, is referred to as a respiration cycle. The airflow can be monitored as exhaled air is warmer, has higher humidity, and contains more water molecules than inhaled air. In addition to breath monitoring, the real-time monitoring of the human skin humidity level via a skin patch can be an important development in prevention of fatal illnesses due to dehydration.

Previously mentioned first transparent and stretchable a rGO/PU sensor was able detect the humidity of the human breath [2]. The device was placed at a distance of 3 cm from the nose, and successfully detected the resistance change between dry air, ambient air and human breath. To test different environments, it was attached to the human finger, providing the feedback on the humidity of the environment, moisture of human skin and dampness of objects. A GO sensor, shown in the top left panel of figure 10, was prepared in an impedance setup and showed ultrafast RRTs of less than 100 ms for thickness of 15 nm, being among the fastest humidity sensors to be reported, comparable to the commercially available optical sensors [68]. It was further tested for speaking, breathing and whistling. The ultrafast performance of these sensors allows the capture of fine features due to moisture modulation during speech. This sensor was also capable of recognizing different whistled tunes, by capturing their distinct patterns characteristic. The patterns were then analyzed using FFT and Principal Components Analysis, resulting in clear clustering for each tune. After training the system with 10 data points per tune, each whistled tune was classified and recognized with an accuracy of approximately 90%, enabling user authentication. A GO/PDDA capacitive sensor was tested for human breath monitoring [62]. The breath response characteristics for a normal adult were measured over 45 s, during which 11 repetitive breathing cycles were observed. The capacitance response showed a sharp increase during exhalation and a drop during inhalation, corresponding to the breathing cycles. Notably, the sensor's response and recovery times were both within 1 s, enabling the capture of fine details related to moisture modulation in human breath. Another GO-based single-layered sensor chip with multiple sensing (figure 9, left panel, middle) was able to monitor human breathing, nose breath and human touch [81]. Because the three different sensors operate independently, as explained in section 3.2.1, they have good sensitivity.

MoS_2 NPs exposed to O_2 plasma were also tested as a human breath sensor and for skin monitoring [93]. The breathing test was conducted with three different conditions, including deep breath, normal

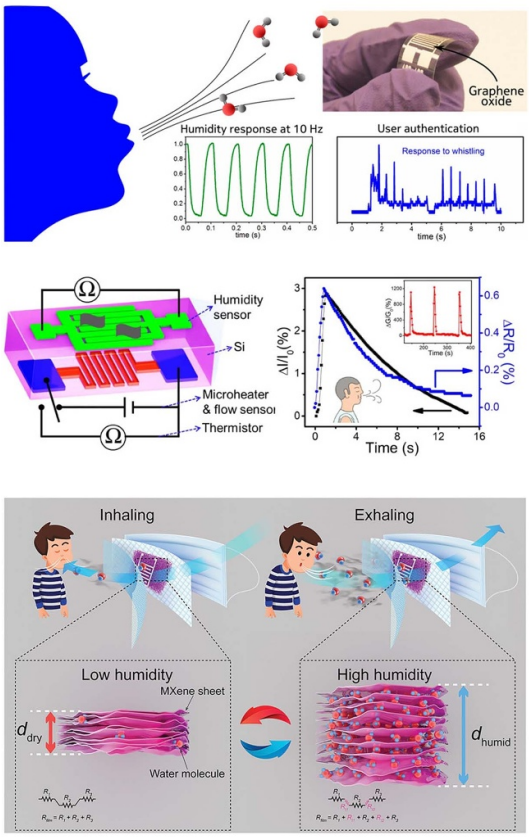

Figure 9. Top: a 15 nm thick GO sensor with the normalized response to a modulated humid airflow at 10 Hz; and a response to ta whistled tune. Reprinted with permission from [68]. Copyright (2013) American Chemical Society. Middle: scheme illustrating the structure of the multifunctional sensor. The GO-based humidity sensor and the microheater/flow/temperature sensor were fabricated on two sides of the Si wafer. Dynamic responses of the flow and temperature sensors to the blow with mouth. Reprinted with permission from [81]. Copyright (2019) American Chemical Society. Bottom: schematic image describing the proposed humidity sensing mechanism of the MXene/TPU sensor. R_1, R_2, and R_3 represent the intrinsic resistance of MXene nanosheets. R_{t1} and R_{t2} represent tunneling resistance at the junctions. R_{flim} represents the total resistance of MXene/TPU composite film. [118] John Wiley & Sons.© 2023 The Authors. Advanced Sensor Research published by Wiley-VCH GmbH.

breath, and fast breath. The breath testing indicated a good response, and the sensor also distinguished wet and dry hands clearly. Inhalation was indicated by the decrease of the resistance, and exhalation by the increase of the resistance.

A sensor based on MXenes with TPU electrospun nanofibers sensors was tested for respiratory monitoring, and embedded into the middle layer of a face mask to avoid the contamination from saliva, as shown in figure 10, left panel, bottom [118]. When a sensing material is added to a flexible and wearable face mask, its resistance has to be stable upon bending. As the MXene nanosheets are abundantly wrapped on the TPU fibers to form a conductive network, the resistance remained stable as the bending angle increased from 0° to 210°, indicating good stability and flexibility. The sensor showed promise for distinguishing different degrees of breathing and accurately monitoring respiratory signals during different physical activities [118]. Another MXenes sensor, combined with GO, successfully detected moisture from human breath and fingertip [71]. MXene/MWCNT-sensing material was drop-coated on pristine fabric and cured by UV light. The electrical circuit was printed by conducting ink and encapsulated by polyimide to avoid short circuiting due to the water vapor. Finally, the whole sensor with the encapsulated circuit was attached inside the mask near the nose as a wearable wireless humidity sensing tag, as shown in figure 9, right panel [119]. The size of the entire tag was 2 cm × 4 cm. The fabric sensor, coupled with a flexible detecting tag, enabled the detection of respiration and the accurate identification of various breathing patterns. It was also able to record respiration signals accurately, even under deformation caused by movement for standing, walking and running. This sensor also provides a practical approach for real-time, wireless respiration monitoring using electronic fabrics.

A flexible humidity sensor, based on SnO_2 thin film, with the food plastic wrap as the substrate material, was integrated into a face mask to detect the breathing pattern [95]. Slow, normal, and fast respiratory patterns were monitored by the real-time current curves, with respiratory rates of 8, 20 and 29 breaths per minute, respectively. Sensor was put inside a glass chamber with a fixed background RH of 70%, 60%, and 50%, and the breath was released 5 cm away from the substrate.

Another fully flexible humidity sensor based on rGO/MoS_2 demonstrated finger proximity detection and non-touch switching [67]. The device was placed at 3 cm away from the human nose. When the breathing rate was 20 breaths per minute (rapid breathing), the device showed a responsivity of 70%. However, at a slower breathing rate of 10 breaths per minute, the responsivity increased to over 90%, demonstrating the good reliability. Water molecules adsorbed and desorbed quickly on the device surface in both rapid and slow breathing modes, resulting in a strong response to human breathing. Additionally, a series of finger proximity detection experiments were conducted in an atmosphere with 46% RH. The results showed that the relative resistance of the device increased gradually from 48.4% to 95.6% as the distance between the finger and the device surface decreased from 2 cm to 0.5 cm. These human respiration and finger proximity measurements demonstrate that the device has potential applications in wearable technology.

A heterojunction made of 3D $MoSe_2$@MoS_2 nanoflowers was positioned at 8 cm from human mouth to monitor respiration, and the finger was positioned

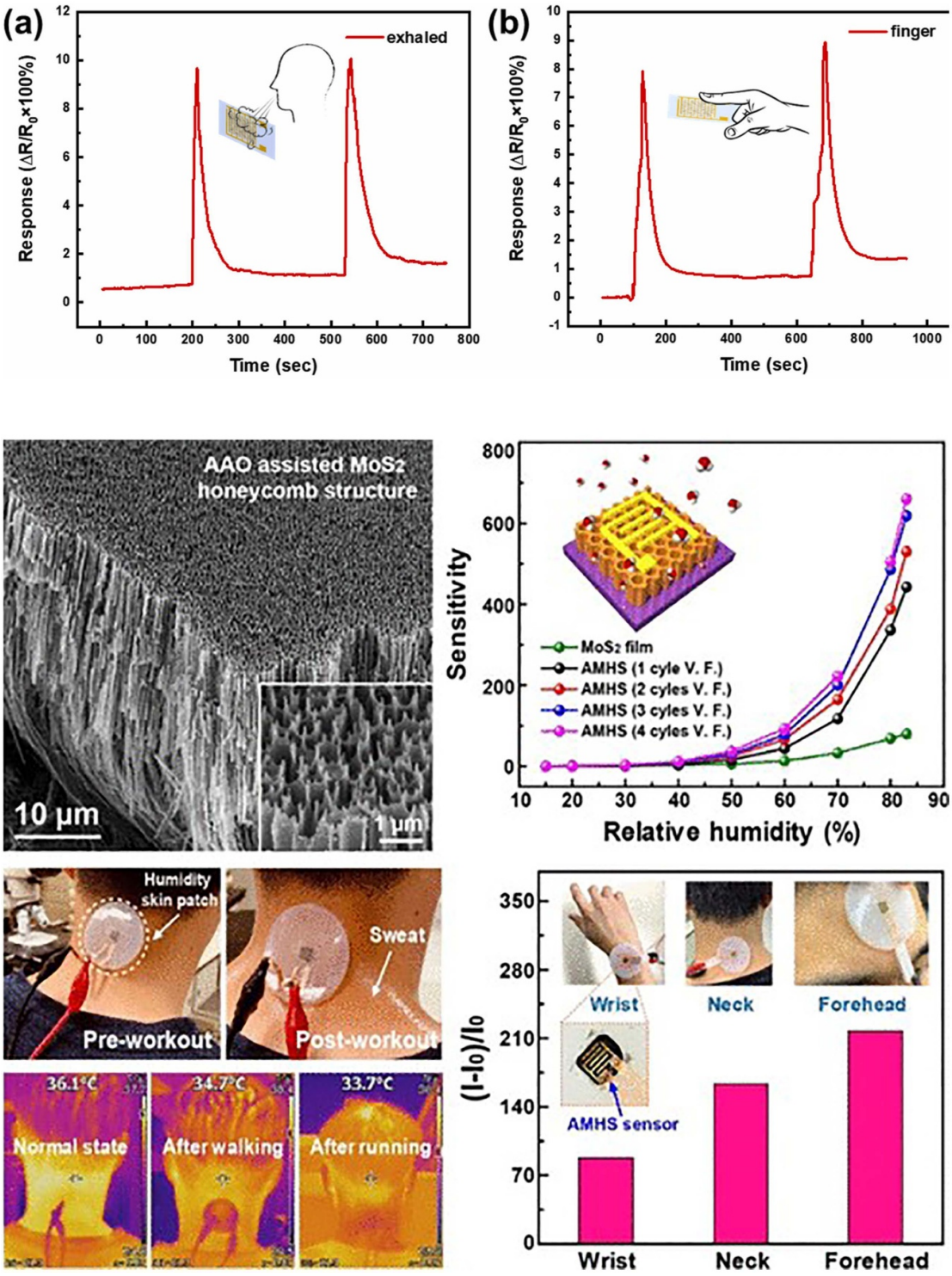

Figure 10. Top panel: (a) the continuous monitoring of the sensor to human deep breath. (b) Repeatability test of the sensor for finger approach distance of 2 cm. Reprinted from [90], Copyright (2024), with permission from Elsevier. Middle panel: FESEM image of the sensor and sensitivity as a function of RH. A bar chart in inset illustrating sensitivity dependence on the RH. Bottom panel: photograph of the attached skin humidity patch on the neck before and after sweating from exercise (top), and the variation in body temperature measured by the IR image camera (bottom). Comparison of the relative current variation in volunteers measured by the skin humidity patch from the neck at different physical conditions. Reprinted with permission from [89]. Copyright (2020) American Chemical Society.

at 2 cm to test for human touch, as shown in the top panel of figure 10 [90]. Both response curves show potential for non-contact detection.

A resistive-type humidity sensor made of a 3D-honeycomb structure based on MoS_2 NTs showed a promising response in humidity in the atmosphere, human breath and human skin in a 20%–85% RH range [89]. As a result, it can be incorporated in multifunctional sensing applications using skin humidity, human respiration pattern and speech

recognition using humidity in exhaled air. These open-ended NTs combined in a honeycomb provide a large number of absorption sites for H_2O molecules. The sensor showed ultrafast RRTs of 0.47 s/0.81 s, respectively, much faster than sensors based on 2D MoS_2. In order to test it in human skin conditions, the sensor was tested in the human body temperature range (31 °C–38 °C) at room RH condition. The sensor showed promise for non-contact applications, as the resistance change was almost negligible when it was placed at 3.8 mm above the heater, showing that it is not affected by the human body temperature, as depicted in the bottom panel of figure 10.

While reducing the MoS_2 flake size leads to formation of S-vacancies as active sites for water molecule absorption, a honeycomb structure contains an even larger number of sites. The absorbed molecules can easily diffuse into the NTs through the open pores, while the defect-rich surface with large number of S-vacancies on the open NT edges, together with the cylindrical shape, allows the water molecules to absorb and assemble easily. In addition, it was assembled into a wearable patch, detecting human skin humidity under different physical conditions and regional sweat rate.

5. Humidity sensors in agriculture

5.1. Soil moisture

Another field of use of humidity sensors is agriculture, as the estimation of soil moisture is of critical importance to avoid over-wetting or water deficiency in order to gain maximal crop production. Sensors based on 2D materials can be utilized as the capacitive devices as they can provide a direct relationship of the soil moisture content and dielectric permittivity of the soil [120]. A device prepared based on MoS_2 sheets showed good sensitivity for both black and red soil, it demonstrated stable performance over 6 months and good reproducibility with response time of 35 s [66]. In another study, a variety of 2D materials were tested as low-cost soil moisture capacitive sensors [121]. The best sensitivity (30%) was reported for MoS_2, following by MoO_3 (13%), GO (11%) and V_2O_5 (9%).

5.2. Plant transpiration monitoring

Efforts have been made to monitor the water status of plants using sensors that can be attached to leaves or placed near plants. However, these sensors with rigid designs often face mechanical incompatibility with the soft surfaces of plant leaves. In this regard, recent advancements in flexible electronics have paved the way for the development of leaf-mounted sensors, which can provide real-time and quantitative information about the water status of plants.

A flexible capacitive-type GO-based humidity sensor with low hysteresis, high sensitivity (3215.25 pF/% RH), and long-term stability was prepared in order to be directly attached onto plant leaves for real-time transpiration tracking [65]. The sensor was fabricated by laser-induced graphene (LIG) interdigital electrode on a PI film, as PI serves as both a precursor for producing LIG and a humidity sensing material. To further improve the sensor's performance, GO was incorporated as the humidity sensing material. The prepared sensor offers excellent flexibility, high sensitivity, and long-term stability, enabling multifunctional applications such as non-contact humidity sensing. Moreover, it can be attached to the surface of leaves without causing any visible damage to plants. By recording capacitance signals, real-time and long-term monitoring of plant transpiration is possible. It can be observed that the capacitance increases 1 d after watering, but over time, it significantly decreases, resembling the pristine condition. However, when the plant was watered again, the capacitance increased accordingly. These findings suggest that the humidity level on the plant surface varies depending on the plant's water conditions. Overall, these results demonstrate that the plant's response to drought can be translated into visible electrical signals, highlighting the potential of the fabricated flexible humidity sensor in the field of intelligent agriculture.

6. Human exposure and environmental impact of 2D materials

The relationship between 2D materials and biological systems is bidirectional, involving interactions where both components influence each other and undergo simultaneous changes. Human exposure to 2D materials falls into three categories: occupational, environmental and biomedical, based on three basic modes of the interactions with biological systems: chemical, mechanical and electronic (see figure 11) [122]. Occupational exposure is already occurring among researchers and is expected to become more significant for workers in nano-manufacturing industries as the field expands. In these settings, workers are primarily exposed to materials in their original synthesized form or as intermediates and byproducts during production processes, highlighting the need to study their biological interactions in these states. In contrast, environmental exposure arises from the unintentional release of these materials, which may undergo chemical transformations before re-entering human systems through air, food or water. Biomedical exposure happens in a somewhat controlled manner and undergoes rigorous investigation through processes which ensure safety, efficacy and biocompatibility before therapeutic applications or medical device approvals. Moreover, synthesis methods play a significant role. Occupational and industrial handling of 2D materials, especially in dry or

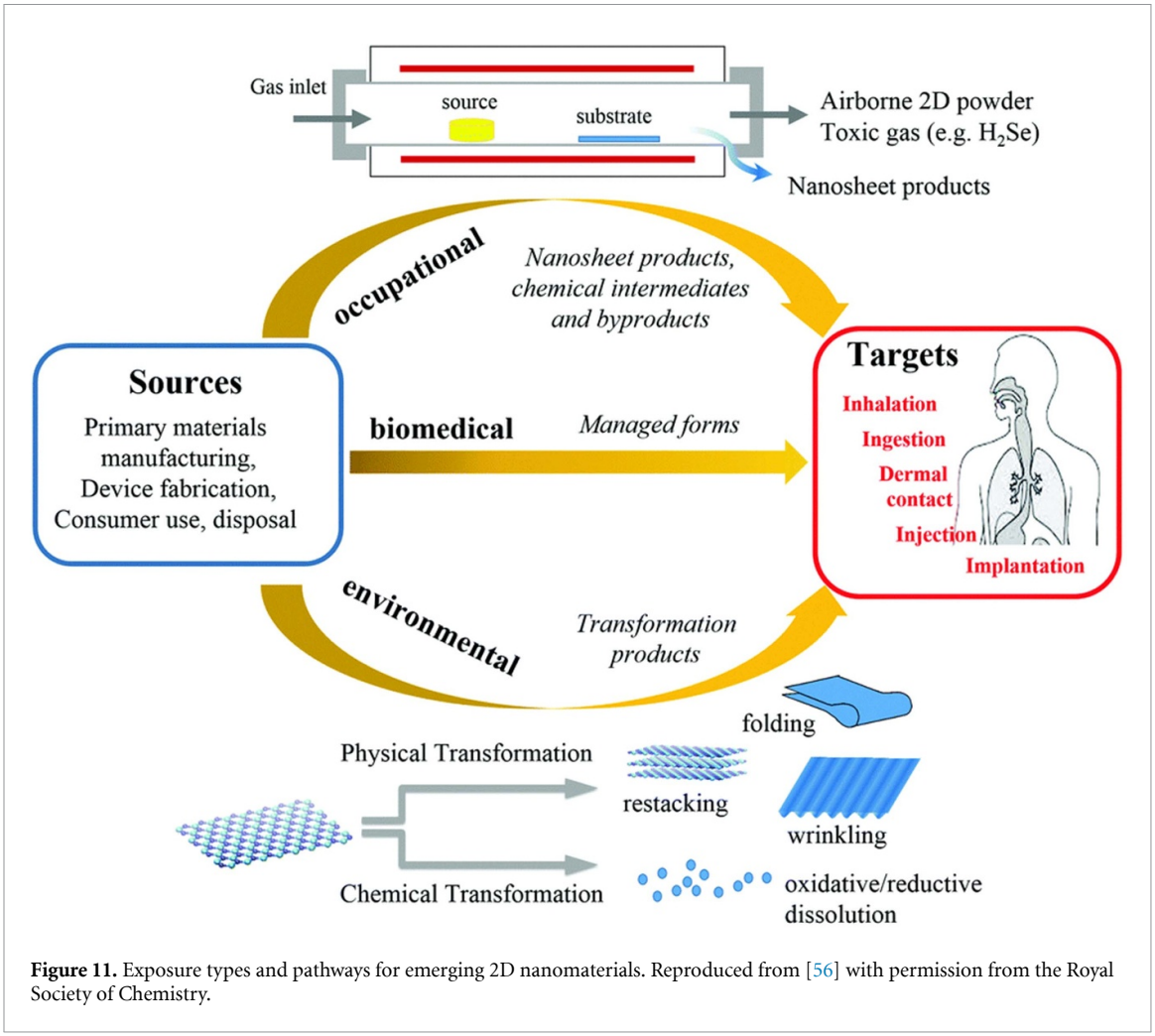

Figure 11. Exposure types and pathways for emerging 2D nanomaterials. Reproduced from [56] with permission from the Royal Society of Chemistry.

powder form, can result in airborne particles that pose inhalation risks and potential deposition into surrounding environment. Aggregation, sedimentation or restacking behaviors of 2D materials in natural systems may further affect their transport and reactivity. However, their widespread adoption is still limited by challenges including large-scale production, long-term durability and economic feasibility. The overall environmental and health risks of engineered nanomaterials are generally low, particularly when strategies like green synthesis and immobilization are applied to reduce exposure [123]. The first in-human study assessing the controlled inhalation of GO on the cardiorespiratory system demonstrated good tolerance without any adverse effects. Blood proteomics revealed minimal changes in plasma protein levels, and only a mild increase in thrombus formation was observed in an *ex vivo* arterial injury model. Overall, short-term exposure to highly purified, ultra-thin GO nanosheets did not result in any significant harm in healthy individuals. These findings support the safe implementation of human exposure studies in clinical settings and provide a foundation for evaluating the biological effects of other two-dimensional nanomaterials [124].

The potential negative impacts of 2D materials remain to be extensively explored, especially as the number of newly synthesized materials continues to grow. Even slight modifications in their composition by, for example, functionalization can significantly alter their physicochemical properties, making the range of possible effects vast and largely unpredictable. The environmental fate of 2D materials is complex due to their diverse chemistries and physical forms. Once released, these materials may undergo chemical (and physical) transformations such as oxidation, sulfidation, aggregation, dissolution, changing chemical state [125, 126] etc, induced by environmental conditions in the presence of atmospheric oxygen, moisture, sunlight and microbial species [127, 128]. Some materials, such as MoS_2, although considered to have low toxicity in bulk, in 2D and nanoscale versions can generate ROS and exhibit dose-dependent cytotoxicity. Moreover, TMDs may degrade and release heavy metals or toxic elements like selenium and tellurium, which are known to accumulate and disrupt biological functions. Their persistence, mobility and interaction with environmental components like soil, water and microbial population raise concerns about long-term

ecological effects. TMDs have been shown to degrade more rapidly under ambient conditions (exposure to air and moisture) compared to graphene-based materials, primarily due to the presence of defect sites and grain boundaries. For instance, MoS_2 undergoes gradual oxidation in air to form MoO_3, and in aqueous environments it further breaks down into soluble MoO_4^{2-} and SO_4^{2-} ions (see figure 3(d)) [128, 129]. Members of the 2D material family do not exhibit uniform resistance to oxidation, and their degradation can occur even at physiologically and environmentally relevant concentrations of oxidative compounds, such as H_2O_2, in both single- and multilayer forms, as observed with pristine graphene [130]. TMDs are also susceptible to H_2O_2-induced oxidation. This oxidative degradation can compromise their electrical, mechanical, and chemical properties, ultimately limiting their effectiveness in environmental applications. Mitigation strategies include procedures such as surface passivation, chemical functionalization and development of protective coatings and nanocomposites. Nanocomposites are particularly interesting due to the synergistic properties they offer [131]. Additionally, surface and interfacial behavior of 2D materials may also be altered by the exposure to common airborne contaminants such as hydrocarbons, water vapor and oxygen. Even at trace levels, they can impact the wettability, electrochemical performance and doping, masking the intrinsic properties of the material (i.e. hydrophobicity of graphene is largely due to adsorbed hydrocarbons rather than its true behavior) [132]. Cracking and quenching (corrosion) occur in MoS_2 and WS_2 after they are stored in the presence of water and oxygen for several months. Recently published research on WS_2 nanotubes found that material stored for a long time in protected atmosphere oxidized only marginally, while other, kept under less controllable conditions suffered severe autocatalytic oxidation [133].

Equally important is the role of these materials in environmental remediation, as a result of synergy between 2D materials and electrochemical methods (electrooxidation and electroreduction) [134, 135]. Their high surface area, tunable surface chemistry and exceptional conductivity is what make them highly effective for removing pollutants from air, water and soil. These applications include the adsorption and absorption of heavy metals, drugs, dyes and other potentially toxic compounds. United Nations' sustainable development goal 6 aims to ensure access to clean water and sanitation for all, a challenge that can be significantly addressed through the innovative use of 2D materials. With their exceptional filtration, sensing, and antimicrobial properties, 2D materials can offer solutions for efficient water purification and real-time quality monitoring [136]. Materials like graphene, MXenes, and TMDs are extensively studied for their role in electrochemical sensing, catalytic degradation of pollutants and fabrication of advanced filtration membranes [137–139]. Notably, MXenes, particularly $Ti_3C_2T_x$, have shown excellent performance in adsorbing heavy metals like Pb^{2+}, Cr^{3+}, and Cd^{2+} due to their rich surface functional groups and high charge capacity. GO and its derivatives are widely used as membranes for water purification, thanks to their ultrahigh water permeability and chemical stability [140, 141]. Degradation of organic pollutants is also possible due to photocatalysis [142, 143]. Environmentally, the use of MoS_2 nanofertilizers reduces dependence on synthetic nitrogen inputs, thereby lowering greenhouse gas emissions and minimizing ecological impact [144]. The vision of clean energy generation is becoming increasingly achievable through the advancement of nanomaterial-based engineering approaches.

7. Outlook and future perspectives

The use of 2D materials in regenerative medicine presents immense potential, but it is held back by critical biocompatibility and toxicity challenges. Factors like size, surface charge and functionalization influence their interaction with biological systems, potentially triggering inflammatory responses, immune reactions or long-term toxicity due to accumulation. Additionally, concerns regarding mechanical stability, controlled drug release, large-scale production, regulatory approval and environmental impact necessitate advanced material engineering and thorough safety assessments to ensure their safe and effective clinical translation [31]. The overall biological impact of 2D materials is strongly governed by their chemical composition, surface characteristics and the extent of exfoliation, all of which shape their interactions with cellular systems. In the case of TMDs, both *in vitro* and *in vivo* studies highlight that their elemental composition, particularly the choice of chalcogen (e.g. sulfur, selenium, tellurium), plays a crucial role in cytotoxicity. Telluride and selenide variants generally elicit more pronounced toxic effects than sulfides, likely due to higher chemical reactivity and chalcogen release [145]. The exfoliation state further modulates bioactivity: nanosheets with high degrees of exfoliation expose more reactive surface area and edge sites, often leading to elevated cellular responses such as oxidative stress and inflammation [146, 147]. Conversely, TMDs that are well-characterized and stably dispersed, especially MoS_2, tend to exhibit lower toxicity profiles and greater biocompatibility, stressing the importance of controlled synthesis and processing in developing safe 2D materials for biomedical and environmental applications [148, 149]. Designing synthesis methods that are not only scalable and cost-effective but

also environmentally sustainable is essential for transitioning from laboratory research to industrial production. Furthermore, addressing the existing gaps in regulatory strategy and standardization is crucial to support the broader commercialization and clinical integration of nanomaterial-based technologies [150].

The previously discussed challenges in the practical utilization, from laboratory research to clinical application, can largely be described as 'cellular response heterogeneity driven by material tunability'. Overcoming these issues requires not only advancements in synthesis/production, standardization and characterization of these materials, but also hand-in-hand progress in SC biology. Recent insights into SC biology have revealed how mechanical and chemical cues from the microenvironment influence cell fate through mechanotransduction pathways [151]. This mechanotransductive signaling integrates the microenvironment, cell membrane, cytoskeleton and nucleus, ultimately guiding SCs behavior and fate. To bridge the gap between controlled laboratory settings and large-scale production, as well as for translation to clinical studies, the development of robust legal frameworks, standards, and protocols is essential. Additionally, mimicking physiological conditions through mathematical modeling, integrated data analysis, and the design of patient-specific therapies will be beneficial to the successful application of 2D materials in regenerative medicine. It offers cost-effective, ethically clean and fast solution [152].

Overall, graphene-based materials pose both risks and opportunities, with toxicity varying based on their form, properties and exposure route. Inhalation can cause lung inflammation, ingestion may disrupt gut microbiota, dermal contact might lead to irritation, and systemic exposure can result in organ accumulation and inflammation. Despite these concerns, graphene shows promise in biomedical applications such as drug delivery, antimicrobial treatments and cancer therapy [153]. Discrepancies that arise between *in vitro* and *in vivo* conditions during the evaluation of nanomaterials and their biocompatibility are the consequences of inability to replicate the complex biological environment of systemic circulation (in comparison to *in vitro* cell culture media). This mismatch, based on how the biomolecular corona differs *in vivo* and *in vitro*, can lead to biases, stressing the importance of the comprehensive approach, using advanced data analyses and machine learning [154]. While no 2D material is universally superior, GO and rGO dominate in bone, cardiac and neural applications due to their conductivity and compatibility. MXenes contribute in cardiac repair and wound healing because of their antioxidative and electroactive nature. TMDs like MoS_2 and WS_2 show great promise in osteogenesis and neuroregeneration due to their semiconducting and photothermal properties, whereas hBN can be considered beneficial in adipogenesis and neural tissue regeneration, (see table 1). The future of regenerative medicine lies in precisely engineering these materials for specific tissue environments while ensuring long-term safety and performance.

In addition, 2D and related materials have become a fertile ground for preparation of a variety of sensors, with the humidity sensing being among the most promising. These sensors can be used in different scenarios, such as for simple monitoring of the RH of the environment, to the human health and agriculture monitoring. In the field of agriculture, these sensors can be utilized to detect soil moisture, or the transpiration cycles of plants, whereby they are coming to a direct contact with the environment. Furthermore, as they can have high stretchability and sensitivity, simple manufacturing process and fast response, they can be added to wearable devices or attached directly to the skin. This is another incentive for studying their biological activity and toxicity, as these novel devices have to be biocompatible if they are to be in contact with human skin and/or soil. This is especially important as the best sensing materials so far are exfoliated or surface modified with reactive surface area and edge sites, which usually leads to elevated cellular response.

In this review, we discussed different sensing mechanisms, and summarized the performance of different families of materials. While the standard types of sensors, such as capacitive and resistive, are relatively easy to fabricate and test, new methods are needed in order to minimize the size and the cost of the sensor. For example, sensors based on fiber optics can be easily integrated into the pre-established fiber optic systems. While developing new sensing mechanisms can lead to improved general performance of the device, another approach is to prepare a material with the best characteristics for the specific need. One way to enhance the sensitivity and RRTs is to increase the density of active edge sites of nanomaterials. This can be achieved via size control, where reducing the size leads to the increase in the density of edge sites. Another approach is shape control, where nanomaterials with unique structures, such as dendrites, nanotubes, NWs and nanoflowers, intrinsically containing a high number of edge sites, improve sensing performance. While rigid sensors based on GO and rGO showed promising characteristics and high RRTs, similar sensors based on or surface-modified or TMDC nanotubes showed superior response. For example, as summarized in table 2, sensor based on plasma-irradiated MoS_2 NPs has a far better performance than MoS_2 sheets, with sub-second RRTs [93]. The best performance was achieved by rGO

functionalized with hydrophilic moieties, with ultrafast RRTs of 25 ms/127 ms [82]. Nevertheless, the stiffness of these materials limits their use for human health sensing.

The increasing need to move away from intrinsically rigid to flexible and wearable sensors requires finding a sensing material that responds well to mechanical deformations through a change in the electrical signal. The best way to achieve flexibility is to combine 2D and TMDC materials with polymer matrices. Some of the most promising candidates are rGO/PU [2], a combined sensing material made of rGO/MoS_2/PI, MXene/GO/COC [71], with the best two reported sensors being MoS_2-based: MoS_2/PEO with RRTs of 0.6 s/0.3 s [88] and MoS_2 NTs/Ecoflex with 0.5 s/0.8 s [89]. Therefore, a good approach to improving the performance of the polymer matrix is to use TMDC nanotubes or NWs. While the CNTs have a good potential, they have a few setbacks as well-they do not disperse well in most organic solvents, resulting in poor homogeneity when mixed with a polymer matrix, so they have to be functionalized in order to enhance the interaction with the solvent. On the other hand, various inorganic TMDC NTs promise a wide spectrum of physical effects beyond the physics of CNTs [155]. They have a high aspect ratio, high specific surface area and excellent mechanical and vibrational/acoustic properties, making them suitable as composite nanofillers as only a small amount can be used for forming a conductive path [156, 157]. The high aspect ratio can also improve the low electrical percolation of the insulating polymer matrix and form an efficient electrical network. Furthermore, MS_2 NTs disperse well in all commonly used solvents, simplifying the composite preparation [158]. As previously mentioned, properly stored WS_2 NTs oxidize only marginally even after more than 20 years [133]. Another family of nanomaterials that shows a great promise as a filler, is the family of metal oxides, as seen in table 2 [159]. Their substoichiometric MO_{3-x} ($0 \leqslant x \leqslant 1$) phases grow in different shapes, such as NWs, flakes, needles and sheets. The optical, electrical and structural properties depend strongly on the degree of the reduction [160]. Together with the already reported sensors on stoichiometric CeO_2 [96], ZnO [97], TiO_2 [98] and SnO_2 NWs [77], W_5O_{14} and $W_{18}O_{49}$, are interesting candidates due to their large aspect ratio, while the presence of photoluminescence and localized surface plasmon resonances can introduce interesting optical effects. Nevertheless, one important aspect that has to be taken into account is the cost, ease of preparation and the field of use of a specific sensor. While some applications require high sensitivity and fast RRT, for some practical uses, such as a quick diagnostic tool outside the hospital setting, the priority should be the cost and the ease of use. For example, 20 breaths per minute is defined as rapid breathing, therefore, a sensor that has a complicated and expensive synthesis method but RRT of microseconds might be superior in performance, but not necessary for practical purposes.

Future health sensing potential of these materials is vast. In addition to devices reviewed here, 2D materials have been slowly incorporated into different types of health sensors. They were reported as respiration sensors for estimation of blood oxygen saturation (SpO_2) [161]. LIG was placed on a PI tape, and this patch-like sensor detected the changes in mechanical deflection (such as chest movement), and measured the respiration rate in real time. Graphene-based biosensors have also been successfully integrated into an automated sensing platform for transporter protein drug delivery, showing to be biocompatible with a picomolar ionic sensitivity [162]. Furthermore, inks made of 2D materials were prepared, compatible with the standard inkjet printing. For example, water-based additive-free ink was prepared from nitrogen-doped carboxylated graphene [163]. This ink was used to fabricate fully inkjet-printed electrodes, which successfully enabled the electrochemical detection of the key neurotransmitter dopamine. The carboxyl groups in NGA ink also enable covalent attachment to biomolecules such as antibodies or aptamers, making it possible to create fully inkjet-printed biosensors.

Overall, 2D and related TMDC materials possess a variety of properties desirable for fabrication of sensors for human health monitoring. Nevertheless, their biological impact has to be thoroughly studied before they can be mass-produced.

Data availability statement

All data that support the findings of this study are included within the article (and any supplementary files).

Acknowledgments

We acknowledge funding provided by the Center for Solid State Physics and New Materials, Institute of Physics Belgrade, through the Grant by the Ministry of Education, Science, and Technological Development of the Republic of Serbia and Center for Solid State Physics and New Materials. BV acknowledges financial support from the Slovenian Research Agency through contract P1-0099. BV acknowledges funding from the European Union's Horizon Europe research and innovation programme under Grant Agreement No. 101185375. This research was also supported by the Science Fund of the Republic of Serbia, 10925, Dynamics of CDW transition in strained quasi-1D systems—DYNAMIQS.

ORCID iDs

Jasmina Lazarević 0000-0001-8980-1688
Bojana Višić 0000-0002-2065-0727

References

[1] Sun X, Guo X, Gao J, Wu J, Huang F, Zhang J-H, Huang F, Lu X, Shi Y and Pan L 2024 E-skin and its advanced applications in ubiquitous health monitoring *Biomedicines* **12** 2307
[2] Trung T Q, Duy L T, Ramasundaram S and Lee N-E 2017 Transparent, stretchable, and rapid-response humidity sensor for body-attachable wearable electronics *Nano Res.* **10** 2021–33
[3] McKinley K L, Longaker M T and Naik S 2023 Emerging frontiers in regenerative medicine *Science* **380** 796–8
[4] Shafiq M, Ali O, Han S-B and Kim D-H 2021 Mechanobiological strategies to enhance stem cell functionality for regenerative medicine and tissue engineering *Front. Cell Dev. Biol.* **9** 747398
[5] Pittenger M F, Discher D E, Péault B M, Phinney D G, Hare J M and Caplan A I 2019 Mesenchymal stem cell perspective: cell biology to clinical progress *npj Regen. Med.* **4** 22
[6] English K P, Mahon B J and Wood K 2014 Mesenchymal stromal cells; role in tissue repair, drug discovery and immune modulation *Concurr. Drug Deliv.* **11** 561–71
[7] Zakrzewski W, Dobrzyński M, Szymonowicz M and Rybak Z 2019 Stem cells: past, present, and future *Stem Cell Res. Ther.* **10** 68
[8] Gokce C, Gurcan C, Delogu L G and Yilmazer A 2022 2D materials for cardiac tissue repair and regeneration *Front. Cardiovasc. Med.* **9** 802551
[9] Qasim M, Chae D S and Lee N Y 2020 Bioengineering strategies for bone and cartilage tissue regeneration using growth factors and stem cells *J. Biomed. Mater. Res. A* **108** 394–411
[10] Hasnain A and Tarasov A 2023 Graphene-based electronic biosensors for disease diagnostics *Graphene Field-Effect Transistors: Advanced Bioelectronic Devices for Sensing Applications ed* O Azzaroni W Knoll (Wiley) pp 71–101
[11] Kostarelos K, Aguilar C and Garrido J A 2024 Clinical translation of graphene-based medical technology *Nat. Rev. Electr. Eng.* **1** 75–76
[12] Sekuła-Stryjewska M, Noga S, Dźwigońska M, Adamczyk E, Karnas E, Jagiełło J, Szkaradek A, Chytrosz P, Boruczkowski D and Madeja Z 2021 Graphene-based materials enhance cardiomyogenic and angiogenic differentiation capacity of human mesenchymal stem cells *in vitro*–focus on cardiac tissue regeneration *Mater. Sci. Eng. C* **119** 111614
[13] Jalilinejad N *et al* 2023 Electrically conductive carbon-based (bio)-nanomaterials for cardiac tissue engineering *Bioeng. Transl. Med.* **8** e10347
[14] Cahill T J, Choudhury R P and Riley P R 2017 Heart regeneration and repair after myocardial infarction: translational opportunities for novel therapeutics *Nat. Rev. Drug Discovery* **16** 699–717
[15] Hu X, Yu S P, Fraser J L, Lu Z, Ogle M E, Wang J-A and Wei L 2008 Transplantation of hypoxia-preconditioned mesenchymal stem cells improves infarcted heart function via enhanced survival of implanted cells and angiogenesis *J. Thoracic Cardiovasc. Surg.* **135** 799–808
[16] Lee W C, Lim C H Y, Shi H, Tang L A, Wang Y, Lim C T and Loh K P 2011 Origin of enhanced stem cell growth and differentiation on graphene and graphene oxide *ACS Nano* **5** 7334–41
[17] Ikram R, Shamsuddin S A A, Mohamed Jan B, Abdul Qadir M, Kenanakis G, Stylianakis M M and Anastasiadis S H 2022 Impact of graphene derivatives as artificial extracellular matrices on mesenchymal stem cells *Molecules* **27** 379
[18] Heo J, Choi J, Kim J Y, Jeong H, Choi D, Han U, Park J H, Park H H and Hong J 2021 2D graphene oxide particles induce unwanted loss in pluripotency and trigger early differentiation in human pluripotent stem cells *J. Hazard. Mater.* **414** 125472
[19] Qi X, Liu Y, Yin X, Zhao R, Zhang W, Cao J, Wang W and Jia W 2023 Surface-based modified 3D-printed BG/GO scaffolds promote bone defect repair through bone immunomodulation *Composites B* **257** 110673
[20] Sulaksono H L S, Annisa A, Ruslami R, Mufeeduzzaman M, Panatarani C, Hermawan W, Ekawardhani S and Joni I M 2024 Recent advances in graphene oxide-based on organoid culture as disease model and cell behavior–a systematic literature review *Int. J. Nanomed.* **19** 6201–28
[21] Romaldini A, Spanò R, Veronesi M, Grimaldi B, Bandiera T and Sabella S 2024 Human multi-lineage liver organoid model reveals impairment of CYP3A4 expression upon repeated exposure to graphene oxide *Cells* **13** 1542
[22] Yu S, Wang L, Chen M, Chen Y and Peng Z 2025 MXene-incorporated conductive hydrogel simulating myocardial microenvironment for cardiac repair and functional recovery *Biomacromolecules* **26** 2378–89
[23] Edrisi F, Baheiraei N, Razavi M, Roshanbinfar K, Imani R and Jalilinejad N 2023 Potential of graphene-based nanomaterials for cardiac tissue engineering *J. Mater. Chem. B* **11** 7280–99
[24] Zaszczyńska A, Zabielski K, Gradys A, Kowalczyk T and Sajkiewicz P 2024 Piezoelectric scaffolds as smart materials for bone tissue engineering *Polymers* **16** 2797
[25] Collins M N, Ren G, Young K, Pina S, Reis R L and Oliveira J M 2021 Scaffold fabrication technologies and structure/function properties in bone tissue engineering *Adv. Funct. Mater.* **31** 2010609
[26] Koons G L, Diba M and Mikos A G 2020 Materials design for bone-tissue engineering *Nat. Rev. Mater.* **5** 584–603
[27] Kang E-S, Kim D-S, Suhito I R, Lee W, Song I and Kim T-H 2018 Two-dimensional material-based bionano platforms to control mesenchymal stem cell differentiation *Biomater. Res.* **22** 10
[28] Yadav S, Singh Raman A P, Meena H, Goswami A G, Bhawna, Kumar V, Jain P, Kumar G, Sagar M and Rana D K 2022 An update on graphene oxide: applications and toxicity *ACS Omega* **7** 35387–445
[29] Soleymani H, Moghaddam M M, Naderi-Manesh H and Taheri R A 2024 Single-layer graphene oxide nanosheets induce proliferation and Osteogenesis of single-cell hBMSCs encapsulated in Alginate Microgels *Sci. Rep.* **14** 25272
[30] Nayak T R, Andersen H, Makam V S, Khaw C, Bae S, Xu X, Ee P-L R, Ahn J-H, Hong B H and Pastorin G 2011 Graphene for controlled and accelerated osteogenic differentiation of human mesenchymal stem cells *ACS Nano* **5** 4670–8
[31] Ma X, Luan Z and Li J 2023 Inorganic nanoparticles-based systems in biomedical applications of stem cells: opportunities and challenges *Int. J. Nanomed.* **18** 143–82
[32] Saikia N 2024 Inorganic-based nanoparticles and biomaterials as biocompatible scaffolds for regenerative medicine and tissue engineering: current advances and trends of development *Inorganics* **12** 292
[33] Liu A, Chen J, Zhang J, Zhang C, Zhou Q, Niu P and Yuan Y 2022 Intra-articular injection of umbilical cord mesenchymal stem cells loaded with graphene oxide granular lubrication ameliorates inflammatory responses and osteoporosis of the subchondral bone in rabbits of modified papain-induced osteoarthritis *Front. Endocrinol.* **12** 822294
[34] Shuai C, Zeng Z, Yang Y, Qi F, Peng S, Yang W, He C, Wang G and Qian G 2020 Graphene oxide assists polyvinylidene fluoride scaffold to reconstruct electrical microenvironment of bone tissue *Mater. Des.* **190** 108564

[35] Zhou X, Sun H and Bai X 2020 Two-dimensional transition metal dichalcogenides: synthesis, biomedical applications and biosafety evaluation *Front. Bioeng. Biotechnol.* **8** 236
[36] Carrow J K, Singh K A, Jaiswal M K, Ramirez A, Lokhande G, Yeh A T, Sarkar T R, Singh I and Gaharwar A K 2020 Photothermal modulation of human stem cells using light-responsive 2D nanomaterials *Proc. Natl Acad. Sci.* **117** 13329–38
[37] Roy S, Deo K A, Singh K A, Lee H P, Jaiswal A and Gaharwar A K 2022 Nano-bio interactions of 2D molybdenum disulfide *Adv. Drug Deliv. Rev.* **187** 114361
[38] Sun G, Yang S, Cai H, Shu Y, Han Q, Wang B, Li Z, Zhou L, Gao Q and Yin Z 2019 Molybdenum disulfide nanoflowers mediated anti-inflammation macrophage modulation for spinal cord injury treatment *J. Colloid Interface Sci.* **549** 50–62
[39] Hadjidemetriou M, Mahmoudi M and Kostarelos K 2024 *In vivo* biomolecule corona and the transformation of a foe into an ally for nanomedicine *Nat. Rev. Mater.* **9** 219–22
[40] Murali A, Lokhande G, Deo K A, Brokesh A and Gaharwar A K 2021 Emerging 2D nanomaterials for biomedical applications *Mater. Today* **50** 276–302
[41] Suhito I R, Han Y, Kim D-S, Son H and Kim T-H 2017 Effects of two-dimensional materials on human mesenchymal stem cell behaviors *Biochem. Biophys. Res. Commun.* **493** 578–84
[42] Natu V, Sokol M, Verger L and Barsoum M W 2018 Effect of edge charges on stability and aggregation of $Ti_3C_2T_z$ MXene colloidal suspensions *J. Phys. Chem. C* **122** 27745–53
[43] Qu X, Guo Y, Xie C, Li S, Liu Z and Lei B 2023 Photoactivated MXene nanosheets for integrated bone–soft tissue therapy: effect and potential mechanism *ACS Nano* **17** 7229–40
[44] Babar Z U D, Iannotti V, Rosati G, Zaheer A, Velotta R, Della Ventura B, Álvarez-Diduk R and Merkoçi A 2025 MXenes in healthcare: synthesis, fundamentals and applications *Chem. Soc. Rev.* **54** 3387–440
[45] Li K, Ji Q, Liang H, Hua Z, Hang X, Zeng L and Han H 2023 Biomedical application of 2D nanomaterials in neuroscience *J. Nanobiotechnol.* **21** 181
[46] Qian Y, Wang X, Song J, Chen W, Chen S, Jin Y, Ouyang Y, Yuan W-E and Fan C 2021 Preclinical assessment on neuronal regeneration in the injury-related microenvironment of graphene-based scaffolds *npj Regen. Med.* **6** 31
[47] Qian Y, Zhao X, Han Q, Chen W, Li H and Yuan W 2018 An integrated multi-layer 3D-fabrication of PDA/RGD coated graphene loaded PCL nanoscaffold for peripheral nerve restoration *Nat. Commun.* **9** 323
[48] da Silva D M, Barroca N, Pinto S C, Semitela Â, de Sousa B M, Martins P A, Nero L, Madarieta I, García-Urkia N and Fernández-San-Argimiro F-J 2023 Decellularized extracellular matrix-based 3D nanofibrous scaffolds functionalized with polydopamine-reduced graphene oxide for neural tissue engineering *Chem. Eng. J.* **472** 144980
[49] Fabbro A, Scaini D, León V, Vázquez E, Cellot G, Privitera G, Lombardi L, Torrisi F, Tomarchio F and Bonaccorso F 2016 Graphene-based interfaces do not alter target nerve cells *ACS Nano* **10** 615–23
[50] Bramini M, Alberini G, Colombo E, Chiacchiaretta M, DiFrancesco M L, Maya-Vetencourt J F, Maragliano L, Benfenati F and Cesca F 2018 Interfacing graphene-based materials with neural cells *Front. Syst. Neurosci.* **12** 358913
[51] Wang Z and Mi B 2017 Environmental applications of 2D molybdenum disulfide (MoS_2) nanosheets *Environ. Sci. Technol.* **51** 8229–44
[52] Zhao C, Deng W and Gage F H 2008 Mechanisms and functional implications of adult neurogenesis *Cell* **132** 645–60
[53] Lee H P and Gaharwar A K 2020 Light-responsive inorganic biomaterials for biomedical applications *Adv. Sci.* **7** 2000863
[54] Wan X, Liu Z and Li L 2021 Manipulation of stem cells fates: the master and multifaceted roles of biophysical cues of biomaterials *Adv. Funct. Mater.* **31** 2010626
[55] Qian Y, Xu Y, Yan Z, Jin Y, Chen X, Yuan W-E and Fan C 2021 Boron nitride nanosheets functionalized channel scaffold favors microenvironment rebalance cocktail therapy for piezocatalytic neuronal repair *Nano Energy* **83** 105779
[56] Merlo A, Mokkapati V, Pandit S and Mijakovic I 2018 Boron nitride nanomaterials: biocompatibility and bio-applications *Biomater. Sci.* **6** 2298–311
[57] Silvestri A, Wetzl C, Alegret N, Cardo L, Hou H-L, Criado A and Prato M 2022 The era of nano-bionic: 2D materials for wearable and implantable body sensors *Adv. Drug Deliv. Rev.* **186** 114315
[58] Ansari H R, Mirzaei A, Shokrollahi H, Kumar R, Kim J-Y, Kim H W, Kumar M and Kim S S 2023 Flexible/wearable resistive gas sensors based on 2D materials *J. Mater. Chem. C* **11** 6528–49
[59] Anwer A H, Saadaoui M, Mohamed A T, Ahmad N and Benamor A 2024 State-of-the-Art advances and challenges in wearable gas sensors for emerging applications: innovations and future prospects *Chem. Eng. J.* **502** 157899
[60] Pawar K K, Kumar A, Mirzaei A, Kumar M, Kim H W and Kim S S 2024 2D nanomaterials for realization of flexible and wearable gas sensors: a review *Chemosphere* **352** 141234
[61] Bi H, Yin K, Xie X, Ji J, Wan S, Sun L, Terrones M and Dresselhaus M S 2013 Ultrahigh humidity sensitivity of graphene oxide *Sci. Rep.* **3** 2714
[62] Zhang D, Tong J, Xia B and Xue Q 2014 Ultrahigh performance humidity sensor based on layer-by-layer self-assembly of graphene oxide/polyelectrolyte nanocomposite film *Sens. Actuators B* **203** 263–70
[63] Yu H-W, Kim H K, Kim T, Bae K M, Seo S M, Kim J-M, Kang T J and Kim Y H 2014 Self-powered humidity sensor based on graphene oxide composite film intercalated by poly (sodium 4-styrenesulfonate) *ACS Appl. Mater. Interfaces* **6** 8320–6
[64] Li N, Chen X, Chen X, Ding X and Zhao X 2017 Ultrahigh humidity sensitivity of graphene oxide combined with Ag nanoparticles *RSC Adv.* **7** 45988–96
[65] Lan L, Le X, Dong H, Xie J, Ying Y and Ping J 2020 One-step and large-scale fabrication of flexible and wearable humidity sensor based on laser-induced graphene for real-time tracking of plant transpiration at bio-interface *Biosens. Bioelectron.* **165** 112360
[66] Siddiqui M S, Mandal A, Kalita H and Aslam M 2022 Highly sensitive few-layer MoS_2 nanosheets as a stable soil moisture and humidity sensor *Sens. Actuators B* **365** 131930
[67] Ke N, Si F, Ma H, Gao Q, Ge G, Liu W, Ding J, Zhang W and Fan X 2024 Fully flexible humidity sensor with fast response and high responsivity based on rGO/MoS_2 for human respiration monitoring and nontouch switches *ACS Appl. Mater. Interfaces* **17** 2317–26
[68] Borini S, White R, Wei D, Astley M, Haque S, Spigone E, Harris N, Kivioja J and Ryhänen T 2013 Ultrafast graphene oxide humidity sensors *ACS Nano* **7** 11166–73
[69] Tamayo A, Danowski W, Han B, Jeong Y and Samorì P 2024 Light-modulated humidity sensing in spiropyran functionalized MoS_2 transistors *Small* 2404633
[70] Ren J, Guo B, Feng Y and Yu K 2020 Few-layer MoS_2 dendrites as a highly active humidity sensor *Physica E* **116** 113782
[71] Waheed W, Anwer S, Khan M U, Sajjad M and Alazzam A 2024 2D $Ti_3C_2T_x$-MXene nanosheets and graphene oxide based highly sensitive humidity sensor for wearable and flexible electronics *Chem. Eng. J.* **480** 147981
[72] Cheng B, Tian B, Xie C, Xiao Y and Lei S 2011 Highly sensitive humidity sensor based on amorphous Al_2O_3 nanotubes *J. Mater. Chem.* **21** 1907–12

[73] Zhang D, Wang D, Zong X, Dong G and Zhang Y 2018 High-performance QCM humidity sensor based on graphene oxide/tin oxide/polyaniline ternary nanocomposite prepared by *in-situ* oxidative polymerization method *Sens. Actuators B* **262** 531–41
[74] Yuan Z, Tai H, Ye Z, Liu C, Xie G, Du X and Jiang Y 2016 Novel highly sensitive QCM humidity sensor with low hysteresis based on graphene oxide (GO)/poly (ethyleneimine) layered film *Sens. Actuators B* **234** 145–54
[75] Lei D, Zhang Q, Liu N, Su T, Wang L, Ren Z, Zhang Z, Su J and Gao Y 2022 Self-powered graphene oxide humidity sensor based on potentiometric humidity transduction mechanism *Adv. Funct. Mater.* **32** 2107330
[76] Luo Y, Chen C, Xia K, Peng S, Guan H, Tang J, Lu H, Yu J, Zhang J and Xiao Y 2016 Tungsten disulfide (WS_2) based all-fiber-optic humidity sensor *Opt. Express* **24** 8956–66
[77] Kuang Q, Lao C, Wang Z L, Xie Z and Zheng L 2007 High-sensitivity humidity sensor based on a single SnO_2 nanowire *J. Am. Chem. Soc.* **129** 6070–1
[78] Guo L *et al* 2012 Two-beam-laser interference mediated reduction, patterning and nanostructuring of graphene oxide for the production of a flexible humidity sensing device *Carbon* **50** 1667–73
[79] Smith A D, Elgammal K, Niklaus F, Delin A, Fischer A C, Vaziri S, Forsberg F, Råsander M, Hugosson H and Bergqvist L 2015 Resistive graphene humidity sensors with rapid and direct electrical readout *Nanoscale* **7** 19099–109
[80] Naik G and Krishnaswamy S 2015 Room-temperature humidity sensing using graphene oxide thin films *Graphene* **5** 1–13
[81] Wu J, Wu Z, Ding H, Wei Y, Yang X, Li Z, Yang B-R, Liu C, Qiu L and Wang X 2019 Multifunctional and high-sensitive sensor capable of detecting humidity, temperature, and flow stimuli using an integrated microheater *ACS Appl. Mater. Interfaces* **11** 43383–92
[82] Anichini C, Aliprandi A, Gali S M, Liscio F, Morandi V, Minoia A, Beljonne D, Ciesielski A and Samorì P 2020 Ultrafast and highly sensitive chemically functionalized graphene oxide-based humidity sensors: harnessing device performances via the supramolecular approach *ACS Appl. Mater. Interfaces* **12** 44017–25
[83] Tripathi S, Gangwar N, Gangwar C and Shukla R 2025 Enhanced humidity sensing using graphene oxide and reduced graphene oxide synthesized via modified Hummers' method *Sens. Imaging* **26** 20
[84] Burman D, Ghosh R, Santra S and Guha P K 2016 Highly proton conducting MoS_2/graphene oxide nanocomposite based chemoresistive humidity sensor *RSC Adv.* **6** 57424–33
[85] Park S Y, Kim Y H, Lee S Y, Sohn W, Lee J E, Shim Y-S, Kwon K C, Choi K S, Yoo H J and Suh J M 2018 Highly selective and sensitive chemoresistive humidity sensors based on rGO/MoS_2 van der Waals composites *J. Mater. Chem. A* **6** 5016–24
[86] Zhang S-L, Choi H-H, Yue H-Y and Yang W-C 2014 Controlled exfoliation of molybdenum disulfide for developing thin film humidity sensor *Curr. Appl Phys.* **14** 264–8
[87] Lou Z, Wu D, Bu K, Xu T, Shi Z, Xu J, Tian Y and Li X 2017 Dual-mode high-sensitivity humidity sensor based on MoS_2/Si nanowires array heterojunction *J. Alloys Compd.* **726** 632–7
[88] Yousaf H Z, Kim S W, Hassan G, Karimov K, Choi K H and Sajid M 2020 Highly sensitive wide range linear integrated temperature compensated humidity sensors fabricated using electrohydrodynamic printing and electrospray deposition *Sens. Actuators B* **308** 127680
[89] Mondal S, Kim S J and Choi C-G 2020 Honeycomb-like MoS_2 nanotube array-based wearable sensors for noninvasive detection of human skin moisture *ACS Appl. Mater. Interfaces* **12** 17029–38
[90] Guo W, He Z, Li J, Yao L, Qiao Y, Wang F, Wang Y and Wang F 2024 3D $MoSe_2$@ MoS_2 heterojunction for humidity sensors to improve sensing performance *J. Alloys Compd.* **983** 173833
[91] Pawbake A S, Waykar R G, Late D J and Jadkar S R 2016 Highly transparent wafer-scale synthesis of crystalline WS_2 nanoparticle thin film for photodetector and humidity-sensing applications *ACS Appl. Mater. Interfaces* **8** 3359–65
[92] Leonardi S, Wlodarski W, Li Y, Donato N, Sofer Z, Pumera M and Neri G 2018 A highly sensitive room temperature humidity sensor based on 2D-WS2 nanosheets *FlatChem* **9** 21–26
[93] Taufik A, Asakura Y, Hasegawa T, Kato H, Kakihana M, Hirata S, Inada M and Yin S 2020 Surface engineering of 1T/2H-MoS_2 nanoparticles by O_2 plasma irradiation as a potential humidity sensor for breathing and skin monitoring applications *ACS Appl. Nano Mater.* **3** 7835–46
[94] Bharatula L D, Erande M B, Mulla I S, Rout C S and Late D J 2016 SnS_2 nanoflakes for efficient humidity and alcohol sensing at room temperature *RSC Adv.* **6** 105421–7
[95] Deb M, Chen M-Y, Chang P-Y, Li P-H, Chan M-J, Tian Y-C, Yeh P-H, Soppera O and Zan H-W 2023 SnO_2-based ultra-flexible humidity/respiratory sensor for analysis of human breath *Biosensors* **13** 81
[96] Fu X, Wang C, Yu H, Wang Y and Wang T 2007 Fast humidity sensors based on CeO_2 nanowires *Nanotechnology* **18** 145503
[97] Kiasari N M, Soltanian S, Gholamkhass B and Servati P 2012 Room temperature ultra-sensitive resistive humidity sensor based on single zinc oxide nanowire *Sens. Actuators A* **182** 101–5
[98] Li Z, Zhang H, Zheng W, Wang W, Huang H, Wang C, MacDiarmid A G and Wei Y 2008 Highly sensitive and stable humidity nanosensors based on LiCl doped TiO_2 electrospun nanofibers *J. Am. Chem. Soc.* **130** 5036–7
[99] Fowler J D, Allen M J, Tung V C, Yang Y, Kaner R B and Weiller B H 2009 Practical chemical sensors from chemically derived graphene *ACS Nano* **3** 301–6
[100] Ma H, Ding J, Zhang Z, Gao Q, Liu Q, Wang G, Zhang W and Fan X 2024 Recent advances in graphene-based humidity sensors with the focus of structural design: a review *IEEE Sens. J.* **24** 20289–311
[101] Buchsteiner A, Lerf A and Pieper J 2006 Water dynamics in graphite oxide investigated with neutron scattering *J. Phys. Chem. A* **110** 22328–38
[102] Nair R, Wu H, Jayaram P N, Grigorieva I V and Geim A 2012 Unimpeded permeation of water through helium-leak–tight graphene-based membranes *Science* **335** 442–4
[103] Wang D-W, Du A, Taran E, Lu G Q M and Gentle I R 2012 A water-dielectric capacitor using hydrated graphene oxide film *J. Mater. Chem.* **22** 21085–91
[104] Late D J *et al* 2013 Sensing behavior of atomically thin-layered MoS_2 transistors *ACS nano* **7** 4879–91
[105] Li H, Yin Z, He Q, Li H, Huang X, Lu G, Fam D W H, Tok A I Y, Zhang Q and Zhang H 2012 Fabrication of single-and multilayer MoS_2 film-based field-effect transistors for sensing NO at room temperature *Small* **8** 63–67
[106] Gobbi M *et al* 2018 Collective molecular switching in hybrid superlattices for light-modulated two-dimensional electronics *Nat. Commun.* **9** 2661
[107] Pujari S *et al* 2024 Au–MoS_2 nanoflowers sensors on interdigitated electrode for monitoring human respiration *Nano Express* (https://doi.org/10.1088/2632-959X/ad6c67)
[108] Wang B, Thukral A, Xie Z, Liu L, Zhang X, Huang W, Yu X, Yu C, Marks T J and Facchetti A 2020 Flexible and stretchable metal oxide nanofiber networks for multimodal and monolithically integrated wearable electronics *Nat. Commun.* **11** 2405
[109] Baloda S, Gupta N and Singh S 2022 A flexible pressure sensor based on multiwalled carbon nanotubes/polydimethylosiloxane composite for wearable

electronic-skin application *IEEE Trans. Electron. Devices* **69** 7011–8
[110] Panth M, Cook B, Alamri M, Ewing D, Wilson A and Wu J Z 2020 Flexible zinc oxide nanowire array/graphene nanohybrid for high-sensitivity strain detection *ACS Omega* **5** 27359–67
[111] Baloda S, Ansari Z A, Singh S and Gupta N 2020 Development and analysis of graphene nanoplatelets (GNPs)-based flexible strain sensor for health monitoring applications *IEEE Sens. J.* **20** 13302–9
[112] Irani F S, Shafaghi A H, Tasdelen M C, Delipinar T, Kaya C E, Yapici G G and Yapici M K 2022 Graphene as a piezoresistive material in strain sensing applications *Micromachines* **13** 119
[113] Xu W, Yang T, Qin F, Gong D, Du Y and Dai G 2019 A sprayed graphene pattern-based flexible strain sensor with high sensitivity and fast response *Sensors* **19** 1077
[114] Ben Aziza Z, Zhang K, Baillargeat D and Zhang Q 2015 Enhancement of humidity sensitivity of graphene through functionalization with polyethylenimine *Appl. Phys. Lett.* **107** 134102
[115] Célérier S *et al* 2018 Hydration of $Ti_3C_2T_x$ MXene: an interstratification process with major implications on physical properties *Chem. Mater.* **31** 454–61
[116] Mirjalali S, Peng S, Fang Z, Wang C H and Wu S 2022 Wearable sensors for remote health monitoring: potential applications for early diagnosis of Covid-19 *Adv. Mater. Technol.* **7** 2100545
[117] Silvestri A *et al* 2023 Ultrasensitive detection of SARS-CoV-2 spike protein by graphene field-effect transistors *Nanoscale* **15** 1076–85
[118] Liu T, Qu D, Guo L, Zhou G, Zhang G, Du T and Wu W 2024 MXene/TPU composite film for humidity sensing and human respiration monitoring *Adv. Sens. Res.* **3** 2300014
[119] Xing H, Li X, Lu Y, Wu Y, He Y, Chen Q, Liu Q and Han R P 2022 MXene/MWCNT electronic fabric with enhanced mechanical robustness on humidity sensing for real-time respiration monitoring *Sens. Actuators B* **361** 131704
[120] SU S L, Singh D N and Baghini M S 2014 A critical review of soil moisture measurement *Measurement* **54** 92–105
[121] Surya S G, Yuvaraja S, Varrla E, Baghini M S, Palaparthy V S and Salama K N 2020 An in-field integrated capacitive sensor for rapid detection and quantification of soil moisture *Sens. Actuators B* **321** 128542
[122] Wang Z, Zhu W, Qiu Y, Yi X, von Dem Bussche A, Kane A, Gao H, Koski K and Hurt R 2016 Biological and environmental interactions of emerging two-dimensional nanomaterials *Chem. Soc. Rev.* **45** 1750–80
[123] Huang X, Auffan M, Eckelman M J, Elimelech M, Kim J-H, Rose J, Zuo K, Li Q and Alvarez P J 2024 Trends, risks and opportunities in environmental nanotechnology *Nat. Rev. Earth Environ.* **5** 572–87
[124] Andrews J P *et al* 2024 First-in-human controlled inhalation of thin graphene oxide nanosheets to study acute cardiorespiratory responses *Nat. Nanotechnol.* **19** 705–14
[125] Garner K L and Keller A A 2014 Emerging patterns for engineered nanomaterials in the environment: a review of fate and toxicity studies *J. Nanopart. Res.* **16** 1–28
[126] Fojtů M, Teo W Z and Pumera M 2017 Environmental impact and potential health risks of 2D nanomaterials *Environ. Sci. Nano* **4** 1617–33
[127] Lin H *et al* 2024 Environmental and health impacts of graphene and other two-dimensional materials: a graphene flagship perspective *ACS Nano* **18** 6038–94
[128] Vranic S, Kurapati R, Kostarelos K and Bianco A 2025 Biological and environmental degradation of two-dimensional materials *Nat. Rev. Chem.* **9** 1–12
[129] Gao J, Li B, Tan J, Chow P, Lu T-M and Koratkar N 2016 Aging of transition metal dichalcogenide monolayers *ACS Nano* **10** 2628–35
[130] Yoo M J and Park H B 2019 Effect of hydrogen peroxide on properties of graphene oxide in Hummers method *Carbon* **141** 515–22
[131] Najmi P, Keshmiri N, Ramezanzadeh M, Ramezanzadeh B and Arjmand M 2023 Epoxy nanocomposites holding molybdenum disulfide decorated with covalent organic framework: all-in-one coatings featuring thermal, UV-shielding, and mechanical properties *Composites B* **260** 110785
[132] Dong W, Dai Z, Liu L and Zhang Z 2024 Toward clean 2D materials and devices: recent progress in transfer and cleaning methods *Adv. Mater.* **36** 2303014
[133] Rosentsveig R, Feldman Y, Kundrat V, Pinkas I, Zak A and Tenne R 2025 Long-term aging of multiwall nanotubes and fullerene-like nanoparticles of WS_2 *J. Solid State Chem.* **346** 125259
[134] Raza S, Hayat A, Bashir T, Chen C, Shen L, Orooji Y and Lin H 2024 Electrochemistry of 2D-materials for the remediation of environmental pollutants and alternative energy storage/conversion materials and devices, a comprehensive review *Sustain. Mater. Technol.* **40** e00963
[135] Yang J *et al* 2022 Oxidations of two-dimensional semiconductors: fundamentals and applications *Chin. Chem. Lett.* **33** 177–85
[136] Arora N K and Mishra I 2022 Sustainable development goal 6: global water security *Environ. Sustain.* **5** 271–5
[137] Garg A, Basu S, Shetti N P and Reddy K R 2021 2D materials and its heterostructured photocatalysts: synthesis, properties, functionalization and applications in environmental remediation *J. Environ. Chem. Eng.* **9** 106408
[138] Zhang C, Ma Y, Zhang X, Abdolhosseinzadeh S, Sheng H, Lan W, Pakdel A, Heier J and Nüesch F 2020 Two-dimensional transition metal carbides and nitrides (MXenes): synthesis, properties, and electrochemical energy storage applications *Energy Environ. Mater.* **3** 29–55
[139] Ikram M, Khan M, Raza A, Imran M, Ul-Hamid A and Ali S 2020 Outstanding performance of silver-decorated MoS_2 nanopetals used as nanocatalyst for synthetic dye degradation *Physica E* **124** 114246
[140] Velusamy S, Roy A, Sundaram S and Kumar Mallick T 2021 A review on heavy metal ions and containing dyes removal through graphene oxide-based adsorption strategies for textile wastewater treatment *Chem. Rec.* **21** 1570–610
[141] Ranjan P *et al* 2024 2D materials for potable water application: basic nanoarchitectonics and recent progresses *Small* **20** 2407160
[142] Junaidi N F D, Othman N H, Fuzil N S, Shayuti M S M, Alias N H, Shahruddin M Z, Marpani F, Lau W J, Ismail A F and Aba N D 2021 Recent development of graphene oxide-based membranes for oil–water separation: a review *Sep. Purif. Technol.* **258** 118000
[143] Perveen H and Zahoor I 2024 Two dimensional materials for wastewater treatment *Int. J. Chem. Biochem. Sci.* **25** 164–77
[144] Li M *et al* 2023 Molybdenum nanofertilizer boosts biological nitrogen fixation and yield of soybean through delaying nodule senescence and nutrition enhancement *ACS Nano* **17** 14761–74
[145] Teo W Z, Chng E L K, Sofer Z and Pumera M 2014 Cytotoxicity of exfoliated transition-metal dichalcogenides (MoS_2, WS_2, and WSe_2) is lower than that of graphene and its analogues *Chemistry A* **20** 9627–32
[146] Latiff N M, Sofer Z, Fisher A C and Pumera M 2017 Cytotoxicity of exfoliated layered vanadium dichalcogenides *Chemistry* **23** 684–90
[147] Chng E L K, Sofer Z and Pumera M 2014 MoS_2 exhibits stronger toxicity with increased exfoliation *Nanoscale* **6** 14412–8
[148] Guiney L M, Wang X, Xia T, Nel A E and Hersam M C 2018 Assessing and mitigating the hazard potential of two-dimensional materials *ACS Nano* **12** 6360–77
[149] Wang X, Mansukhani N D, Guiney L M, Ji Z, Chang C H, Wang M, Liao Y P, Song T B, Sun B and Li R 2015 Differences in the toxicological potential of 2D versus

aggregated molybdenum disulfide in the lung *Small* **11** 5079–87
[150] Baig N, Kammakakam I and Falath W 2021 Nanomaterials: a review of synthesis methods, properties, recent progress, and challenges *Mater. Adv.* **2** 1821–71
[151] Ferrai C and Schulte C 2024 Mechanotransduction in stem cells *Eur. J. Cell Biol.* **103** 151417
[152] Lu B *et al* 2024 When machine learning meets 2D materials: a review *Adv. Sci.* **11** 2305277
[153] Volkov Y, McIntyre J and Prina-Mello A 2017 Graphene toxicity as a double-edged sword of risks and exploitable opportunities: a critical analysis of the most recent trends and developments *2D Mater.* **4** 022001
[154] Castagnola V, Tomati V, Boselli L, Braccia C, Decherchi S, Pompa P P, Pedemonte N, Benfenati F and Armirotti A 2024 Sources of biases in the *in vitro* testing of nanomaterials: the role of the biomolecular corona *Nanoscale Horiz.* **9** 799–816
[155] Višić B, Panchakarla L S and Tenne R 2017 Inorganic nanotubes and fullerene-like nanoparticles at the crossroads between solid-state chemistry and nanotechnology *J. Am. Chem. Soc.* **139** 12865–78
[156] Evarestov R, Kovalenko A, Bandura A, Domnin A and Lukyanov S 2018 Comparison of vibrational and thermodynamic properties of MoS_2 and WS_2 nanotubes: first principles study *Mater. Res. Express* **5** 115028
[157] Sedova A, Višić B, Vega-Mayoral V, Vella D, Gadermaier C, Dodiuk H, Kenig S, Tenne R, Gvishi R and Bar G 2020 Silica aerogels as hosting matrices for WS_2 nanotubes and their optical characterization *J. Mater. Sci.* **55** 1–12
[158] Yadgarov L *et al* 2018 Strong light–matter interaction in tungsten disulfide nanotubes *Phys. Chem. Chem. Phys.* **20** 20812–20
[159] Pirker L and Višić B 2022 Recent progress in the synthesis and potential applications of two-dimensional tungsten (Sub) oxides *Isr. J. Chem.* **62** e202100074
[160] Višić B, Pirker L, Opačić M, Milosavljević A, Lazarević N, Majaron B and Remškar M 2022 Influence of crystal structure and oxygen vacancies on optical properties of nanostructured multi-stoichiometric tungsten suboxides *Nanotechnology* **33** 275705
[161] Madevska Bogdanova A, Koteska B, Vićentić T, Ilić S D, Tomić M, Spasenović M and Michel C 2024 Blood oxygen saturation estimation with laser-induced graphene respiration sensor *J. Sens.* **2024** 4696031
[162] Meincke M *et al* 2025 Integration of highly sensitive large-area graphene-based biosensors in an automated sensing platform *Measurement* **240** 115592
[163] Nalepa M-A, Panáček D, Dědek I, Jakubec P, Kupka V, Hrubý V, Petr M and Otyepka M 2024 Graphene derivative-based ink advances inkjet printing technology for fabrication of electrochemical sensors and biosensors *Biosens. Bioelectron.* **256** 116277